JOC The Journal of Organic Chemistry

pubs.acs.org/joc Article

Stable Axially Chiral Isomers of Arylnaphthalene Lignan Glycosides with Antiviral Potential Discovered from *Justicia procumbens*

Yang Zhao, Chuen-Fai Ku, Xin-Ya Xu, Nga-Yi Tsang, Yu Zhu, Chen-Liang Zhao, Kang-Lun Liu, Chuang-Chuang Li, Lijun Rong, and Hong-Jie Zhang*

Cite This: *J. Org. Chem.* 2021, 86, 5568−5583 Read Online

ACCESS | Metrics & More | Article Recommendations | Supporting Information

ABSTRACT: Arylnaphthalene lignans (ANLs) were known to have axial chirality due to the biphenyl skeleton with hindered rotation at the single bond. However, the stable ANL atropisomers have not been isolated from nature until the present study. Phytochemical separation of the methanol extract of the stems and barks of *Justicia procumbens* led to the isolation of 11 ANL glycosides including four pairs of new atropisomers with stable confirmations at room temperature. Their structures were deduced from elucidation of the extensive spectral data, and their absolute configurations were determined by the circular dichroism, electronic circular dichroism, and X-ray methods as well as the total synthesis of one pair of the atropisomers. The ANL compounds were evaluated for their antiviral potential, and it was found that they displayed great antiviral activity discrepancy between a pair of atropisomers due to the geometric orientation. The 1′***P***-oriented atropisomers showed much more significant antiviral potency than their corresponding 1′***M***-oriented counterparts. The biological activity discrepancy caused by the axial chirality will not only inspire synthetic design of novel ANL atropisomers to enrich the structural diversity, but also provide important hints to direct the synthetic approaches toward the antiviral drug development of ANL compounds.

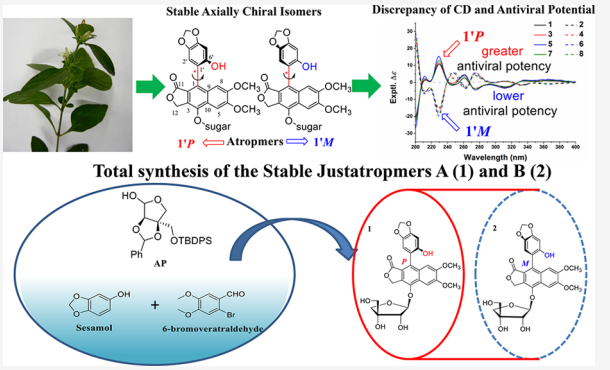

Downloaded via UNIV OF CONNECTICUT on May 15, 2021 at 03:07:16 (UTC).
See https://pubs.acs.org/sharingguidelines for options on how to legitimately share published articles.

INTRODUCTION

Arylnaphthalene lignans (ANLs) belong to aryltetralin lignan compounds with the carbon skeleton containing a naphthalene bonded with a phenyl or a substituted phenyl group. They abundantly exist as the characteristic secondary metabolites in the plants of *Justicia* sp. (Acanthaceae).[1] The genus is rich in medicinal plants that have been used for the treatment of fever, pain, and diarrhea in China and around the Southern Asian countries. ANL compounds are found to possess extensive biological activities, such as anticancer, anti-inflammation, and antiplatelet activities,[2−4] and some of them were demonstrated to be promising lead molecules for antiviral drug development.[5−8]

ANLs are generally believed to have axial chirality due to the biphenyl skeleton with a hindered rotation around the sp^2-sp^2 σ bond.[9] Many quantum theories have been involved to describe the phenomenon of the biphenyl axial chirality of ANLs to form atropisomers. Charlton and his colleagues studied the hindered rotation phenomenon in 1996 and 1997, and they adopted a computer simulation technique to determine the enantiomerization barrier of some arynaphthalenes.[10,11] According to their calculations, separation of the axially chiral biphenyl stereoisomers at room temperature normally requires energy barriers of 22−23.3 kcal/mol.[12−16] However, to best of our knowledge, the coexistence of a stable pair of ANL atropisomers in the nature have not been obtained at room temperature until the present report.

Pharmacological activity discrepancy due to atropisomerization has been investigated for its application in drug development.[17−21] ANL compounds have been known for their high antiviral activities,[5−8] and the atropisomerization could be useful characteristic property to increase their development potential as clinically used drugs through exploiting structure diversity and bioactivity specificity.

Among the naturally occurring ANLs,[1,22] only a few of them, including 6′-hydroxyl justicidins A and B from *J. procumbens*, were found to contain oxygenated groups at C-6′.[23] Although 6′-hydroxyl justicidins A and B were not reported to have axial chirality, the presence of the oxy-substituted group at C-6′ did raise the possibility of having axial chirality potential. We hypothesize that, with a functional group substituted at C-6′ in

Received: January 10, 2021
Published: April 5, 2021

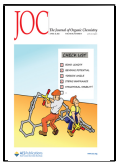

© 2021 American Chemical Society

https://doi.org/10.1021/acs.joc.1c00068
J. Org. Chem. 2021, 86, 5568−5583

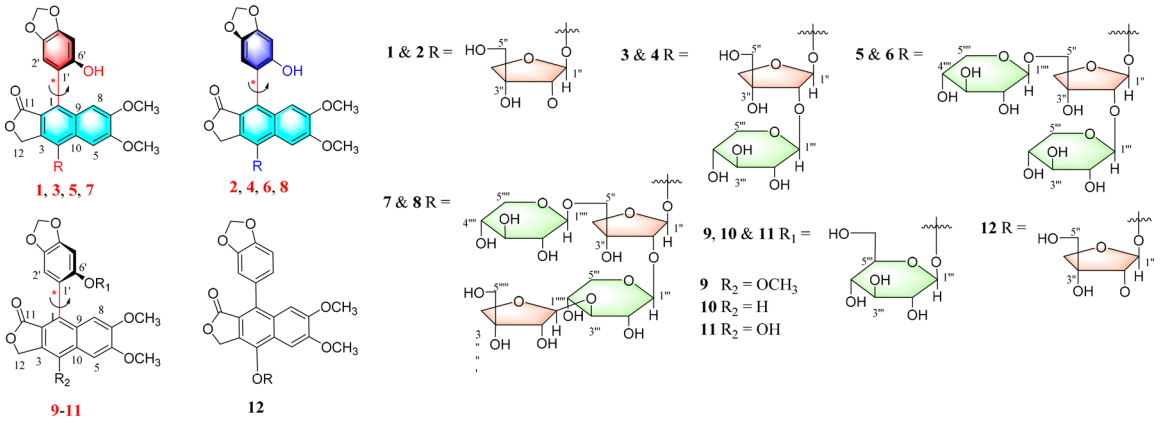

Figure 1. Structures of compounds **1**−**12**.

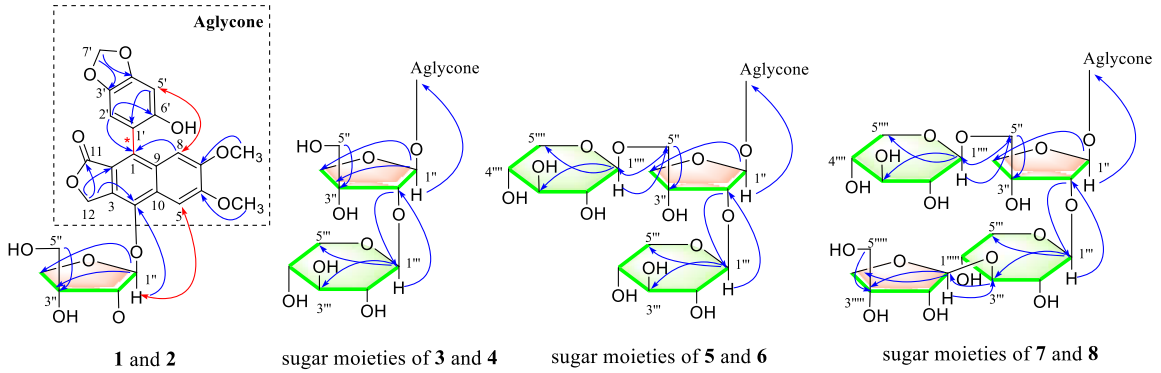

Figure 2. Key HMBC (blue arrow), COSY (green line) and NOESY (red arrow) correlations of **1**, **2** and the glycosides of compounds **3**−**8**.

the phenyl moiety of ANLs, the energy barrier may be increased significantly enough to prevent a free rotation around the C−C single bond due to the steric hindrance caused by the interaction between the C-6′ group and the carbonyl carbon of the γ-lactone group, which could produce stable atropisomers at room temperature. The computer simulation[24−26] further made the prediction that the stable atropisomer of 6′-hydroxyl justicidin B should exist at room temperature as the axial rotation barrier energy of this compound was estimated based on a relaxed scan and calculated as 34.8 kcal/mol (Figures S1A−S1C). More accurate prediction of the rotational barriers was carried out by further optimization of the rotational transition state structures (Figures S1D−S1E). The barrier energies were found to be 26.3 and 26.5 kcal/mol for the atropisomers of 6′-hydroxyl justicidin B and the aglycone atropisomers, respectively, which are higher than the needed energy (23.3 kcal/mol) to overcome the axial rotation barrier. The prediction result gives a significant theoretical support for the hypothesis that the stable atropisomer of a C-6′-substituted ANL compound should be able to exist in the nature.

In the search for novel anti-HIV compounds, we have carried out systematic phytochemical investigation of the stems and barks of the medicinal plant *J. procumbens*, guided by the "One-Stone-Two-Birds" antiviral evaluation assay[6,27] and thin layer chromatography (TLC) using chloride ferric as the color developing reagent to detect phenolic compounds. As a result, we isolated four pairs of new ANL glycosides, which are named as justatropmers A−H (**1**−**8**). All eight compounds are substituted with 6′-hydroxy in their structures. This is the first report for obtaining pairs of stable ANL atropisomers from the nature, which confirmed our earlier hypothesis. Moreover, an additional new [justatropmer I (**11**)] and two known [justprocumbenosides B (**9**) and C (**10**)] were also obtained from this plant (Figure 1). The structures of these compounds were deduced based on the extensive interpretation of the spectral data, and their absolute configurations were determined by the circular dichroism (CD) and electronic circular dichroism (ECD) methods. All of the natural compounds were evaluated for their antiviral potential, and the results showed that there was a great discrepancy of the bioactivity between a pair of atropisomers.

To further confirm the structure accuracy of the natural atropisomers elucidated through the spectral analysis, we successfully prepared compounds **1** and **2** through a concise *de novo* total synthesis route without using the costly and complex chiral catalysts. The synthetic **1** and **2**, their isomerized apioside congeners **23** and **24**, and the intermediates **15**, **19**, **20**, and **21** were also subjected to antiviral activity evaluation.

Herein, we report the isolation, structural elucidation, total synthesis, and biological activity evaluation of the ANLs due to their atropisomerism.

RESULTS AND DISCUSSION

Isolation and Structure Elucidation of Justatropmers.

Compound **1** was isolated as white amorphous powders. Its molecular formula was determined to be $C_{26}H_{24}O_{12}$ by the analysis of the HR-ESI-MS (*m*/*z* 529.1377 $[M + H]^+$, calcd $C_{26}H_{25}O_{12}$, 529.1346) and NMR data. The UV spectrum with prominent absorption pattern at λ_{max} 202, 266, and 310 nm and

https://doi.org/10.1021/acs.joc.1c00068
J. Org. Chem. 2021, 86, 5568−5583

Table 1. Spectral Data of Justatropmers A (1) and B (2)

^{1}H (400 MHz) and ^{13}C (100 MHz) NMR Data in CD_3OD (δ, ppm, J, Hz)						
	1			2		
position	δ_H (J, Hz)	δ_C, type	key HMBC correlations	δ_H (J, Hz)	δ_C, type	key HMBC correlations
1		133.80, C			133.85, C	
2		120.95, C			120.95, C	
3		130.10, C			130.31, C	
4		146.28, C			146.23, C	
5	7.643, s	101.89, CH	C-4, C-6, C-7, C-9	7.652, s	101.85, CH	C-4, C-6, C-7, C-9
6		153.11, C			153.14, C	
7		151.54, C			151.55, C	
8	7.041, s	107.19, CH	C-1, C-6, C-7, C-10	7.051, s	107.17, CH	C-1, C-6, C-7, C-10
9		131.92, C			131.93, C	
10		128.29, C			128.32, C	
11		172.25, C			172.26, C	
12	5.476, d, (15.1)	68.77, CH_2	C-2, C-4, C-11	5.473, d, (15.1)	68.79, CH_2	C-2, C-4, C-11
	5.549, d, (15.1)			5.549, d, (15.1)		
6-OCH_3	3.988, s	56.45, CH_3	C-6	4.001, s	56.45, CH_3	C-6
7-OCH_3	3.743, s	56.01, CH_3	C-7	3.749, s	56.00, CH_3	C-7
1′		114.70, C			114.70, C	
2′	6.532, s	98.89, CH	C-4′, C-6′	6.543, s	98.90, CH	C-4′, C-6′
3′		142.12, C			142.11, C	
4′		149.75, C			149.75, C	
5′	6.527, s	111.48, CH	C-1′, C-3′	6.538, s	111.40, CH	C-1′, C-3′
6′		150.76, C			150.83, C	
7′	5.934, d (1.0)	102.48, CH_2	C-3′, C-4′	5.943, d (1.0)	102.49, CH_2	C-3′, C-4′
	5.958, d (1.0)			5.966, d (1.0)		
1″	5.515, d (3.6)	112.69, CH	C-4, C-3″, C-4″	5.514, d (3.6)	112.83, CH	C-4, C-3″, C-4″
2″	4.506, d (3.6)	78.68, CH	C-3″, C-4″	4.512, d (3.6)	78.69, CH	C-3″, C-4″
3″		80.31, C	C-1″, C-5″		80.31, C	C-1″, C-5″
4″	3.921, d (9.7)	75.91, CH_2	C-1″, C-2″	3.929, d (9.7)	75.89, CH_2	C-1″, C-2″
	4.325, d (9.7)			4.345, d (9.7)		
5″	3.667, d (11.4)	64.26, CH_2	C-3″	3.672, d (11.4)	64.23, CH_2	C-3″
	3.708, d (11.4)			3.713, d (11.4)		

HR-ESI-MS, molecular formula, UV, IR, CD data and sugar linkages		
	1	2
HR-ESI-MS	m/z 529.1377 $[M + H]^+$, calcd 529.1346	m/z 529.1375 $[M + H]^+$, calcd 529.1346
MW	$C_{26}H_{25}O_{12}$	$C_{26}H_{25}O_{12}$
UV (MeOH)	λ_{max} (log ε): 202 (2.98), 229 (2.76), 266 (3.08), 310 (sh) (2.53), 359 (sh) (2.09) nm	λ_{max} (log ε): 201 (3.00), 229 (2.78), 262 (3.11), 310 (sh) (2.57), 360 (sh) (2.10) nm
IR (KBr)	ν_{max}: 3434, 2920, 1746, 1624, 1507, 1482, 1458, 1456, 1434, 1384, 1355, 1263, 1242, 1215, 1167, 1105, 1066, 1035, 993, 934, 858, 769 cm^{-1}	ν_{max}: 3440, 2927, 1747, 1626, 1508, 1482, 1456, 1434, 1395, 1355, 1264, 1243, 1215, 1167, 1104, 1067, 1036, 993, 934, 858, 770 cm^{-1}
sugar linkages	4-*O*-β-D-apiofuranosyl	4-*O*-β-D-apiofuranosyl
CD (MeOH)	λ ($\Delta\varepsilon$): 200 (−20.98), 212 (1.32), 217 (0.67), 229 (10.69), 245 (−1.62), 261 (2.61), 274 (−3.60), 294 (−1.01), 312 (−2.59), 332 (0.63) nm	λ ($\Delta\varepsilon$): 200 (22.24), 211 (−5.72), 218 (−3.64), 229 (−15.37), 246 (2.65), 263 (−3.16), 275 (4.04), 297 (−0.19), 313 (0.78), 331 (−1.34), 349 (−0.45) nm

the IR absorption bands at 3434 cm^{-1} (hydroxy group), 1746 cm^{-1} (ester group), 1624 cm^{-1} (conjugated carbonyl group) and 934 cm^{-1} (methylenedioxy group) of **1** were shown to be similar to those of the ANLs described in the literature,[3,28] indicating that **1** has an arylnaphthalene nucleus with a γ-lactone ring group. In the HMBC spectrum of **1**, the two proton signals at δ_H 5.476 and 5.549 were found to have the correlations with C-4 (δ_C 146.28) (Figure 2), which assigned the γ-lactone carbonyl carbon at C-11 rather than at C-12. Further analysis of the 1D and 2D NMR data of **1** revealed that the compound has a very similar structure with the reported known compound tuberculatin (**12**).[29] Compound **1** differs from **12** only by the disappearance of an aryl ABX chemical shift system that was observed in the ^{1}H NMR spectrum of **12**. Instead, the ^{1}H NMR spectrum of **1** showed two singlet aromatic protons at δ_H 6.532 (1H, s) and 6.527 (1H, s) (Table 1), which suggested an extra oxygenated group substituted at C-6′ in the 1-aryl group of **1**. In combination with the analysis of the ^{13}C NMR and HMBC spectral data, the oxy-group at C-6′ was characterized as a hydroxyl. The anomeric proton [δ_H 5.515 (1H, d, J = 3.6 Hz)] and carbon (δ_C 111.48) chemical shifts were found to be similar to those of **12**, revealing the existence of a β-D-apiose sugar moiety in **1**, which was confirmed by comparing the acidically hydrolyzed sugar of **1** with the authentic sugar sample. The long-range correlation from δ_H 5.515 to δ_C146.28 observed in the HMBC spectrum of **1** assigned the β-D-apiose moiety at C-4 (Figure 2). Accordingly, **1** is determined as 4-*O*-β-D-apiofuranosyl-6′-hydroxydiphyllin and is given the trivial name of justatropmer A.

https://doi.org/10.1021/acs.joc.1c00068
J. Org. Chem. 2021, 86, 5568−5583

Compound **2** was isolated as white amorphous powders using an HPLC separation technique. In HPLC chromatography, the eluting peak of **2** appeared at a different retention time from that of **1**. However, its NMR spectral data were found to be almost identical to those of **1** except for some slight different chemical shifts in the 1D NMR data (Table 1), suggesting that **2** had the same planar ANL structure as **1**. Compound **2** is therefore also determined as 4-*O*-*β*-D-apiofuranosyl-6′-hydroxydiphyllin and was given the trivial name of justatropmer B. The difference between the two structures was caused by the stereochemistry due to the orientation of the presence of a hydroxyl group at C-6′ position, which resulted in the highly hindered aryl−aryl bond rotation between C-1 and C-1′. Because of this significantly enhanced aryl−aryl bond rotation barrier, compounds **1** and **2** were able to be separated as a stable pair of atropisomers at room temperature. The presence of the carbonyl group at C-11 may also contribute to the thermal stability of the pair of the atropisomers due to its interaction with the C-6′ hydroxy group.

The aglycones of **1** and **2** are, in fact, a pair of enantiomers. By attaching a steric sugar moiety, the aglycone enantiomers turned them as a pair of diastereoisomers, which could be separated by using an achiral reverse phase column. The HPLC analysis of **1** and **2** on a chiral column (CHIRALPAK IA-3) yielded only one peak, respectively, indicating each of them being isolated as a pure compound. This was the first time to confirm the existence of stable atropisomers of ANLs in the nature at room temperature. Although there is a sugar moiety with flexible and versatile conformations attached to the ANL core skeleton at the C-4, the sugar unit is away from the C-1 and C-1′ rotation bond with a long distance and is thus not taken into consideration when the axial rotation of the ANL aglycone is calculated for its barrier energy in a steric model. The planar structure of the aglycone of **1** and **2** is the same as that of 6′-hydroxyl justicidin B, and the bond rotation energy barrier of C-2−C-1−C-1′−C-2′ of the aglycone is estimated as 34.8 kcal/mol (Figure S1B,C), which is higher than the barrier energy (22−23.3 kcal/mol) required for separation of a pair of stable biphenyl atropisomers at room temperature.[12−14]

The CD spectra of compounds **1** and **2** were used to determine their absolute configurations. A pair of simplified model compounds (1′***P***-aglycone and 1′***M***-aglycone) were introduced to distinguish the pair of atropisomers (Figure 3). The geometry optimization calculations were performed at B3LYP/6-31G(d) in MeOH (methanol) by the default IEFPCM solvation model with dispersion correction (GD3). A frequency calculation with the same level of theory was conducted to confirm the optimized structures with energy-minimized confirmations.[30−32] The TD-DFT calculations of 1′***P*** and 1′***M***-aglycones were performed with M06-2X/def2TZVP, and the experimental CD spectra of **1** and **2** were found to be consistent with the calculated ECD spectra of 1′***P***-aglycone and 1′***M***-aglycone, respectively (Figure 3). The absolute configurations of the aglycone isomers of **1** and **2** are thus determined as 1′***P*** (i.e., ***R***) and 1′***M*** (i.e., ***S***), respectively.

Although compounds **1** and **2** exist as stable atropisomers at room temperature (25 °C), we further measured the temperatures that could trigger the conversion between the two atropisomers. A solution containing compound **1** or **2** was heated at a temperature of 37, 57, 77, or 97 °C for 1 h, and the solution was then analyzed by UHPLC on an achiral reversed-phase column. The results showed that both compounds were able to overcome the rotation barrier energy of the C-1 and C-1′ bond by being converted to their respective atropisomers at a temperature of 97 °C (Figure 4). However, no conversion between the two atropisomers was observed under 77 °C, indicating that the atropisomers were stable at the temperatures below 77 °C. The rotational barriers for aglycone computed at room temperature are $\Delta H^{\ddagger}$ = 25.3 kcal/mol, $\Delta S^{\ddagger}$ = −3.9 cal/mol·K, and $\Delta G^{\ddagger}$ = 26.5 kcal/mol. The relatively small value of $\Delta S^{\ddagger}$ indicates a negligible influence of temperature on the values of $\Delta G^{\ddagger}$. The approximate 3:1 ratio after 1 h at 97 °C indicates a $t_{1/2}$ for racemization of 1.7 h, which corresponds to a

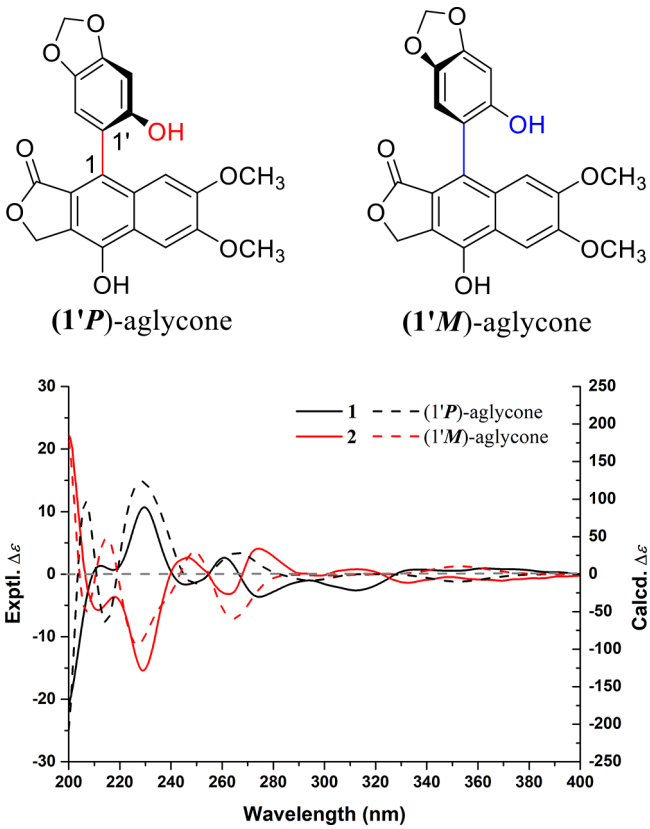

Figure 3. Experimental CD spectra for **1** and **2** and the calculated ECDs for 1′***P***-aglycone (shift = +8 nm) and 1′***M***-aglycone (shift = +9 nm) and their model compounds.

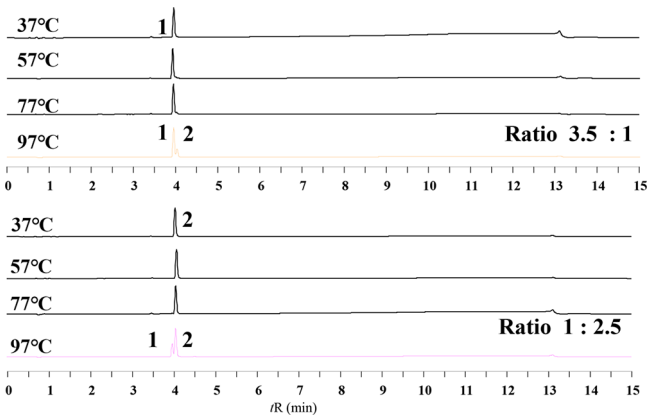

Figure 4. UHPLC analysis of the stability of **1** and **2** heated at different temperatures.

https://doi.org/10.1021/acs.joc.1c00068
J. Org. Chem. 2021, 86, 5568−5583

Table 2. Spectral Data of Justatropmers C (3) and D (4)

^{1}H (400 MHz) and ^{13}C (100 MHz) NMR Data in CD_3OD (δ, ppm, J, Hz)						
	3			4		
position	δ_H (J, Hz)	δ_C, type	key HMBC correlations	δ_H (J, Hz)	δ_C, type	key HMBC correlations
1		133.98, C			133.84, C	
2		121.05, C			120.90, C	
3		130.34, C			130.66, C	
4		146.10, C			145.88, C	
5	7.666, s	102.09, CH	C-4, C-6, C-7, C-9	7.587, s	102.47, CH	C-4, C-6, C-7, C-9
6		153.25, C			153.17, C	
7		151.64, C			151.52, C	
8	7.074, s	107.32, CH	C-1, C-6, C-7, C-10	7.023, s	153.17, CH	C-1, C-6, C-7, C-10
9		132.05, C			131.86, C	
10		128.26, C			128.16, C	
11		172.21, C			172.15, C	
12	5.479, d (15.1)	68.84, CH_2	C-2, C-4, C-11	5.475, d (15.1)	68.83, CH_2	C-2, C-4, C-11
	5.544, d (15.1)			5.516, d (15.1)		
6-OCH_3	4.026, s	56.81, CH_3	C-6	4.007, s	56.81, CH_3	C-6
7-OCH_3	3.757, s	56.03, CH_3	C-7	3.740, s	56.00, CH_3	C-7
1′		114.75, C			114.63, C	
2′	6.544, s	98.93, CH	C-4′, C-6′	6.471, s	98.90, CH	C-4′, C-6′
3′		142.18, C			142.05, C	
4′		149.79, C			149.72, C	
5′	6.579, s	111.41, CH	C-1′, C-3′	6.524, s	111.41, CH	C-1′, C-3′
6′		150.78, C			150.77, C	
7′	5.949, d (1.0)	102.51, CH_2	C-3′, C-4′	5.935, d (1.0)	102.47, CH_2	C-3′, C-4′
	5.970, d (1.0)			5.959, d (1.0)		
1″	5.664, d (2.7)	111.35, CH	C-4, C-3″, C-4″	5.626, d (2.7)	111.46, CH	C-4, C-3″, C-4″
2″	4.715, d (2.7)	85.97, CH	C-3″, C-4″, C-1‴	4.724, d (2.7)	85.94, CH	C-3″, C-4″, C-1‴
3″		81.24, C	C-1″, C-5″		81.22, C	C-1″, C-5″
4″	3.911, d (9.7)	75.69, CH_2	C-1″, C-2″	3.907, d (9.7)	75.64, CH_2	C-1″, C-2″
	4.323, d (9.7)			4.329, d (9.7)		
5″	3.667, d (11.4)	64.11, CH_2	C-3″	3.776, d (11.4)	64.13, CH_2	C-3″
	3.720, d (11.4)			3.729, d (11.4)		
1‴	4.534, d (7.5)	106.17, CH	C-2″, C-5‴, C-3‴	4.543, d (7.5)	106.10, CH	C-2″, C-5‴, C-3‴
2‴	3.296, m	75.20, CH	C-4‴, C-3‴	3.363, m	75.19, CH	C-4‴, C-3‴
3‴	3.369, m	77.67, CH	C-1‴, C-5‴	3.387, m	77.65, CH	C-1‴, C-5‴
4‴	3.471, m	71.08, CH	C-5‴, C-2‴	3.473, m	71.07, CH	C-5‴, C-2‴
5‴	3.245, dd (10.5, 11.4)	67.29, CH_2	C-1‴, C-3‴	3.269, dd (10.5, 11.4)	67.25, CH_2	C-1‴, C-3‴
	3.808, dd (5.3, 11.4)			3.845, dd (5.3, 11.4)		

HR-ESI-MS, molecular formula, UV, IR, CD Data, And Sugar Linkages		
	3	4
HR-ESI-MS	m/z 661.1805 $[M + H]^+$, calcd 661.1769, m/z 529.1367 $[M + H - 132]^+$	m/z 661.1805 $[M + H]^+$, calcd 661.1769
MW	$C_{31}H_{32}O_{16}$	$C_{31}H_{32}O_{16}$
UV (MeOH)	λ_{max} (log ε): 200 (2.86), 229 (2.63), 266 (2.97), 310 (sh) (2.42), 361 (sh) (2.00) nm	λ_{max} (log ε): 202 (3.09), 229 (2.86), 265 (3.17), 310 (sh) (2.63), 359 (sh) (2.17) nm
IR (KBr)	ν_{max}: 3414, 2932, 1745, 1625, 1508, 1484, 1456, 1435, 1385, 1342, 1264, 1244, 1216, 1167, 1123, 1054, 1037, 993, 934, 858, 769 cm^{-1}	ν_{max}: 3400, 2927, 1745, 1625, 1508, 1484, 1456, 1436, 1386, 1341, 1264, 1244, 1216, 1168, 1123, 1053, 992, 935, 859, 768 cm^{-1}
sugar linkages	4-*O*-[*β*-D-xylopyranosyl-(1→2)-*β*-D-apiofuranosyl]	4-*O*-[*β*-D-xylopyranosyl-(1→2)-*β*-D-apiofuranosyl]
CD (MeOH)	λ ($\Delta\varepsilon$): 200 (−22.84), 212 (1.74), 217 (0.40), 229 (11.53), 245 (−0.62), 262 (4.37), 274 (−3.46), 292 (−1.19), 311 (−3.07), 334 (0.95) nm	λ ($\Delta\varepsilon$): 200 (26.93), 211 (−6.27), 218 (−3.28), 229 (−17.54), 248 (5.24), 264 (−2.48), 275 (5.52), 298 (−0.36), 310 (0.47), 332 (−1.56), 348 (−0.21) nm

$\Delta G^{\ddagger}$ for racemization of ∼28 kcal/mol according to Erying equation.[33] This agrees well with the DFT-computed $\Delta G^{\ddagger}$ of 26.5 kcal/mol (Figure S1E).

Compounds **3**−**8** were given the trivial names of justatropmers C−H, respectively, and their structures were determined as 4-*O*-[*β*-D-xylopyranosyl-(1→2)-*β*-D-apiofuranosyl]-6′-hydroxydiphyllin for the atropisomers **3** and **4**, 4-*O*-[bis-*β*-D-xylopyranosyl-(1→2, 1→5)-*β*-D- apiofuranosyl]-6′-hydroxydiphyllin for the atropisomers **5** and **6**, and 4-*O*-{[*β*-D-apiofuranosyl-(1→3)-*β*-D-xylopyranosyl-(1→2)][*β*-D-xylopyranosyl-(1 → 5)]-*β*-D-apiofuranosyl}-6′-hydroxydiphyllin for the atropisomers **7** and **8** according to the HR-ESI-MS and comprehensive NMR data (Tables 2−4). The sugar units contained in these atropisomers were confirmed by comparison of their hydrolyzed sugars with the corresponding authentic samples. Their absolution stereochemistry was determined by the CD spectral analysis (Figure 5). The absolute configurations of **3**, **5**, and **7** were determined as 1′***P*** (i.e., ***R***) while **4**,

https://doi.org/10.1021/acs.joc.1c00068
J. Org. Chem. 2021, 86, 5568−5583

Table 3. Spectral Data of Justatropmers E (5) and F (6)

	^{1}H (400 MHz) and ^{13}C (100 MHz) NMR Data in CD_3OD (δ, ppm, J, Hz)					
	5			**6**		
position	δ_H (J, Hz)	δ_C, type	key HMBC correlations	δ_H (J, Hz)	δ_C, type	key HMBC correlations
1		134.14, C			133.86, C	
2		121.08, C			120.79, C	
3		130.65, C			131.01, C	
4		146.18, C			145.77, C	
5	7.634, s	102.13, CH	C-4, C-6, C-7, C-9	7.457, s	101.67, CH	C-4, C-6, C-7, C-9
6		153.33, C			153.13, C	
7		151.69, C			151.44, C	
8	7.062, s	107.38, CH	C-1, C-6, C-7, C-10	6.989, s	107.19, CH	C-1, C-6, C-7, C-10
9		132.11, C			131.75, C	
10		128.29, C			128.04, C	
11		172.23, C			172.12, C	
12	5.452, d (15.1)	68.89, CH_2	C-2, C-4, C-11	5.449, d (15.1)	68.83, CH_2	C-2, C-4, C-11
	5.521, d (15.1)			5.369, d (15.1)		
6-OCH_3	4.013, s	56.93, CH_3	C-6	5.958, s	56.86, CH_3	C-6
7-OCH_3	3.748, s	56.04, CH_3	C-7	3.726, s	56.01, CH_3	C-7
1′		114.78, C			114.56, C	
2′	6.543, s	98.52, CH	C-4′, C-6′	6.520, s	98.93, CH	C-4′, C-6′
3′		142.22, C			141.97, C	
4′		149.83, C			149.71, C	
5′	6.580, s	111.42, CH	C-1′, C-3′	6.533, s	111.60, CH	C-1′, C-3′
6′		150.81, C			150.78, C	
7′	5.944, d (1.0)	102.51, CH_2	C-3′, C-4′	5.941, d (1.0)	102.52, CH_2	C-3′, C-4′
	5.966, d (1.0)			5.964, d (1.0)		
1″	5.610, d (2.9)	111.58, CH	C-4, C-3″, C-4″	5.518, d (2.9)	111.78, CH	C-4, C-3″, C-4″
2″	4.791, d (2.9)	86.91, CH	C-3″, C-4″, C-1‴	4.783, d (2.9)	87.10, CH	C-3″, C-4″, C-1‴
3″		80.11, C	C-1″, C-5″		80.07, C	C-1″, C-5″
4″	3.931, d (9.7)	75.65, CH_2	C-1″, C-2″	3.924, d (9.7)	75.61, CH_2	C-1″, C-2″
	4.281, d (9.7)			4.250, d (9.7)		
5″	3.726, d (10.4)	71.89, CH_2	C-3″, C-1⁗	3.709, d (10.4)	72.37, CH_2	C-3″, C-1⁗
	4.052, d (10.4)			4.070, d (10.4)		
1‴	4.653, d (7.6)	105.73, CH	C-2″, C-5‴, C-3‴	4.700, d (7.6)	105.32, CH	C-2″, C-5‴, C-3‴
2‴	3.292, m	75.29, CH	C-4‴, C-3‴	3.293, m	75.24, CH	C-4‴, C-3‴
3‴	3.362, m	77.77, C	C-1‴, C-5‴	3.382, m	77.79, C	C-1‴, C-5‴
4‴	3.463, m	71.16, CH_2	C-5‴, C-2‴	3.464, m	71.17, CH_2	C-5‴, C-2‴
5‴	3.234, dd (10.5, 11.4)	67.30, CH_2	C-1‴, C-3‴	3.254, dd (10.5, 11.4)	67.23, CH_2	C-1‴, C-3‴
	3.797, dd (5.3, 11.4)			3.829, dd (5.3, 11.4)		
1⁗	4.341, d (7.6)	105.64, CH	C-5″, C-3⁗, C-5⁗	4.343, d (7.6)	105.48, CH	C-5″, C-3⁗, C-5⁗
2⁗	3.312, m	74.93, CH	C-4⁗, C-3⁗	3.369, m	74.91, CH	C-4⁗, C-3⁗
3⁗	3.359, m	77.79, CH	C-1⁗, C-5⁗	3.359, m	77.68, CH	C-1⁗, C-5⁗
4⁗	3.520, m	71.22, CH	C-5⁗, C-2⁗	3.550, m	71.11, CH	C-5⁗, C-2⁗
5⁗	3.261, dd (10.5, 11.4)	67.15, CH_2	C-1⁗, C-3⁗	3.284, dd (10.5, 11.4)	67.09, CH_2	C-1⁗, C-3⁗
	3.901, dd (5.3, 11.4)			3.923, dd (5.3, 11.4)		

	HR-ESI-MS, molecular formula, UV, IR data and sugar linkages	
	5	**6**
HR-ESI-MS	m/z 793.2219 $[M + H]^+$, calcd for 793.2191	m/z 793.2244 $[M + H]^+$, calcd for 793.2191
MW	$C_{36}H_{40}O_{20}$	$C_{36}H_{40}O_{20}$
UV (MeOH)	λ_{max} (log ε): 200 (2.86), 225 (2.64), 260 (2.97), 307 (sh) (2.44), 355 (sh) (2.19) nm	λ_{max} (log ε): 202 (2.86), 228 (2.64), 262 (2.97), 309 (sh) (2.44), 362 (sh) (2.19) nm
IR (KBr)	ν_{max}: 3410, 2927, 1745, 1625, 1508, 1484, 1454, 1436, 1389, 1344, 1264, 1244, 1216, 1168, 1052, 993, 938, 858, 769 cm^{-1}	ν_{max}: 3410, 2923, 1744, 1625, 1508, 1484, 1455, 1436, 1385, 1342, 1264, 1244, 1216, 1168, 1052, 993, 938, 860, 769 cm^{-1}
sugar linkages	4-*O*-[*bis*-*β*-D-xylopyranosyl-(1→2, 1→5)-*β*-D-apiofuranosyl]	4-*O*-[*bis*-*β*-D-xylopyranosyl-(1→2, 1→5)-*β*-D-apiofuranosyl]
CD (MeOH)	λ ($\Delta\varepsilon$): 200 (−27.24), 211 (3.46), 218 (0.82), 229 (15.28), 246 (−1.05), 261 (4.59), 275 (−4.40), 292 (−1.32), 311 (−3.49), 334 (1.41) nm	λ ($\Delta\varepsilon$): 200 (29.36), 211 (−6.93), 218 (−4.61), 229 (−19.86), 246 (5.92), 262 (−3.66), 275 (5.62), 296 (0.09), 313 (0.70), 332 (−1.69), 348 (−0.30) nm

6, and **8** were determined as 1′***M*** (i.e., ***S***). The 1′***P*** stereochemistry of **5** was further confirmed by the X-ray crystallographic data acquired with Cu radiation using the Flack parameter (Figure S5), which reveals that the TDDFT calculations for absolute configurations of these atropisomers can yield reliable results.

In terms of the planar structures, compounds **9** and **10** were identified as the same as the known justicidinosides B and C,

https://doi.org/10.1021/acs.joc.1c00068
J. Org. Chem. 2021, 86, 5568−5583

Table 4. Spectral Data of Justatropmers G (7) and H (8)

^{1}H (400 MHz) and ^{13}C (100 MHz) NMR Data in CD_3OD (δ, ppm, J, Hz)						
	7			8		
position	δ_H (J, Hz)	δ_C, type	key HMBC correlations	δ_H (J, Hz)	δ_C, type	key HMBC correlations
1		134.08, C			133.92, C	
2		121.08, C			120.92, C	
3		130.50, C			130.79, C	
4		146.19, C			145.94, C	
5	7.672, s	102.17, CH	C-4, C-6, C-7, C-9	7.551, s	101.88, CH	C-4, C-6, C-7, C-9
6		153.31, C			153.21, C	
7		151.68, C			151.55, C	
8	7.076, s	107.36, CH	C-1, C-6, C-7, C-10	7.022, s	107.26, CH	C-1, C-6, C-7, C-10
9		132.09, C			131.88, C	
10		128.25, C			128.13, C	
11		172.22, C			172.15, C	
12	5.470, d, (15.1)	68.88, CH_2	C-2, C-4, C-11	5.429, d, (15.1)	68.87, CH_2	C-2, C-4, C-11
	5.541, d, (15.1)			5.493, d, (15.1)		
6-OCH_3	4.031, s	56.94, CH_3	C-6	3.993, s	56.91, CH_3	C-6
7-OCH_3	3.755, s	56.03, CH_3	C-7	3.742, s	56.02, CH_3	C-7
1′		114.77, C			114.64, C	
2′	6.541, s	98.94, CH	C-4′, C-6′	6.522, s	98.94, CH	C-4′, C-6′
3′		142.21, C			142.06, C	
4′		149.82, C			149.75, C	
5′	6.583, s	111.49, CH	C-1′, C-3′	6.526, s	111.53, CH	C-1′, C-3′
6′		150.79, C			150.82, C	
7′	5.946, d (1.0)	102.51, CH_2	C-3′, C-4′	5.945, d (1.0)	102.51, CH_2	C-3′, C-4′
	5.967, d (1.0)			5.967, d (1.0)		
1″	5.637, d (2.8)	111.42, CH	C-4, C-3″, C-4″	5.577, d (2.8)	111.60, CH	C-4, C-3″, C-4″
2″	4.805, d (2.8)	86.76, CH	C-3″, C-4″, C-1‴	4.795, d (2.8)	86.85, CH	C-3″, C-4″, C-1‴
3″		80.11, C	C-1″, C-5″		80.51, C	C-1″, C-5″
4″	3.928, d (10.0)	75.60, CH_2	C-1″, C-2″	3.930, d (10.0)	75.78, CH_2	C-1″, C-2″
	4.305, d (10.0)			4.284, d (10.0)		
5″	3.739, d (10.5)	71.72, CH_2	C-3″, C-1⁗	3.731, d (10.5)	71.99, CH_2	C-3″, C-1⁗
	4.041, d (10.5)			4.051, d (10.5)		
1‴	4.636, d (7.6)	105.79, CH	C-2″, C-5‴, C-3‴	4.656, d (7.6)	105.58, CH	C-2″, C-5‴, C-3‴
2‴	3.303, m	75.27, CH	C-4‴, C-3‴	3.296, m	75.26, CH	C-4‴, C-3‴
3‴	3.441, m	84.89, C	C-1‴, C-5‴, C-1⁗′	3.451, m	84.95, C	C-1‴, C-5‴, C-1⁗′
4‴	3.447, m	71.15, CH_2	C-5‴, C-2‴	3.468, m	71.14, CH_2	C-5‴, C-2‴
5‴	3.251, dd (10.5, 11.4)	67.29, CH_2	C-1‴, C-3‴	3.250, dd (10.5, 11.4)	67.26, CH_2	C-1‴, C-3‴
	3.775, dd (5.3, 11.4)			3.825, dd (5.3, 11.4)		
1⁗	4.362, d (7.6)	105.48, CH	C-5″, C-3⁗, C-5⁗	4.361, d (7.6)	105.46, CH	C-5″, C-3⁗, C-5⁗
2⁗	3.435, m	74.53, CH	C-4⁗, C-3⁗	3.462, m	74.52, CH	C-4⁗, C-3⁗
3⁗	3.368, m	77.75, CH	C-1⁗, C-5⁗	3.364, m	77.89, CH	C-1⁗, C-5⁗
4⁗	3.560, m	69.94, CH	C-5⁗, C-2⁗	3.586, m	69.91, CH	C-5⁗, C-2⁗,
5⁗	3.270, dd (10.5, 11.4)	66.80, CH_2	C-1⁗, C-3⁗	3.271, dd (10.5, 11.4)	66.79, CH_2	C-1⁗, C-3⁗
	3.939, dd (5.3, 11.4)			3.950, dd (5.3, 11.4)		
1⁗′	5.315, d (2.8)	111.17, CH	C-3‴, C-3⁗′, C-4⁗′	5.321, d (2.8)	111.13, CH	C-3‴, C-3⁗′, C-4⁗′
2⁗′	4.016, d (2.8)	77.91, CH	C-3⁗′, C-4⁗′	4.014, d (2.8)	77.78, CH	C-3⁗′, C-4⁗′
3⁗′		80.51, C	C-1⁗′, C-5⁗′		80.10, C	C-1⁗′, C-5⁗′
4⁗′	3.798, d (10.0)	75.03, CH_2	C-2⁗′, C-1⁗′	3.810, d (10.0)	75.00, CH_2	C-2⁗′, C-1⁗′
	4.140, d (10.0)			4.145, d (10.0)		
5⁗′	3.612, s	65.18, CH_2	C-3⁗′	3.615, s	65.14, CH_2	C-3⁗′

HR-ESI-MS, molecular formula, UV, IR data, and sugar linkages		
	7	8
HR-ESI-MS	m/z 947.2494 $[M + Na]^+$, Calcd for 947.2428	m/z 947.2493 $[M + Na]^+$, Calcd for 947.2428
M.W.	$C_{41}H_{48}O_{24}$	$C_{41}H_{48}O_{24}$
UV (MeOH)	λ_{max} (log ε): 200 (3.20), 228 (2.98), 262 (3.31), 309 (sh) (2.78), 362 (sh) (2.27) nm	λ_{max} (log ε): 202 (3.00), 228 (2.76), 260 (3.10), 309 (sh) (2.54), 359 (sh) (2.27) nm
IR (KBr)	ν_{max}: 3427, 2926, 1746, 1626, 1507, 1483, 1436, 1390, 1345, 1264, 1244, 1214, 1168, 1054, 994, 938, 858, 769 cm^{-1}	ν_{max}: 3430, 2964, 1745, 1626, 1508, 1484, 1436, 1384, 1341, 1262, 1245, 1216, 1168, 1053, 994, 939, 801, 769 cm^{-1}
sugar linkages	4-O-{[β-D-apiofuranosyl-(1→3)-β-D-xylopyranosyl-(1→2)][β-D-xylopyranosyl-(1→5)]-β-D-apiofuranosyl}	4-O-{[β-D-apiofuranosyl-(1→3)-β-D-xylopyranosyl-(1→2)][β-D-xylopyranosyl-(1→5)]-β-D-apiofuranosyl}

https://doi.org/10.1021/acs.joc.1c00068
J. Org. Chem. 2021, 86, 5568−5583

Table 4. continued

	HR-ESI-MS, molecular formula, UV, IR data, and sugar linkages	
	7	**8**
CD (MeOH)	λ ($\Delta\varepsilon$): 200 (−23.39), 210 (2.31), 218 (0.33), 229 (12.88), 248 (−1.19), 260 (3.86), 275 (−3.60), 293 (−0.70), 313 (−2.84), 333 (0.64) nm	λ ($\Delta\varepsilon$): 200 (28.16), 210 (−5.2), 219 (−2.85), 229 (−18.81), 248 (5.87), 262 (−3.39), 275 (5.02), 296 (−0.27), 315 (0.99), 331 (−1.74), 343 (−0.48) nm

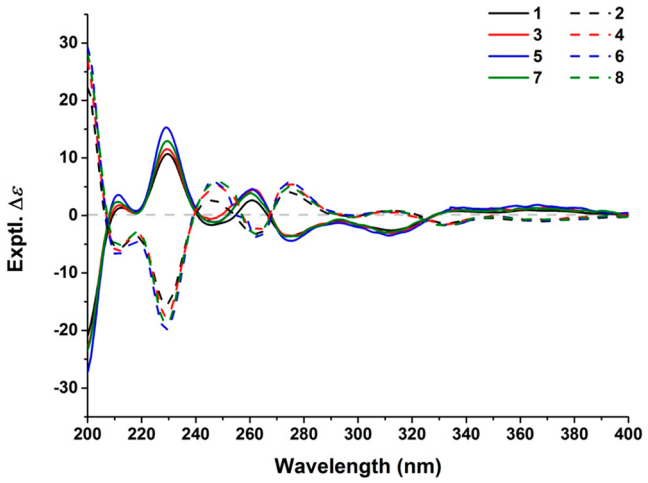

Figure 5. Experimental CD spectra for **1**−**8**.

respectively, by comparing their spectral data with those of the literature (Table 5).[5] Because they contain a β-D-glucose moiety substituted at the C-6′ position, the two compounds should exist as a stable state of one form of their atropisomers. However, we did not isolate their corresponding atropisomers, neither did the literature report them.

The molecular formula of compound **11** was deduced from the analysis of HR-ESI-MS (m/z 543.1351 $[M + H]^+$, calcd 543.1497) and NMR data as $C_{27}H_{26}O_{12}$. The comparison of the NMR data of **11** with **9** and **10** (Table 5) revealed that **11** possessed the very similar structure as **9** and **10** except for the different substituents at C-4. In the ^{1}HNMR spectra, the observed proton signals of δ_H 7.739 in **10** disappeared in **9** and **11**. In addition, the carbon signal at δ_C 119.71 observed in the ^{13}C NMR spectrum of **10** was significantly downshifted to δ_C 148.99 and δ_C 146.35 in the ^{13}C NMR spectra of **9** and **11**, respectively, indicating that **9** and **11** have an oxy group substituted at C-4. Considering the elemental compositions, the oxy groups of **9** and **11** were determined as methoxy and hydroxy groups, respectively. Thus, the new compound of **11** is identified as 6′-*O*-β-D-glucopyranosyldiphyllin, and is given the trivial name of justatropmer I.

Compounds **9**−**11** contain a β-D-glucose moiety at C-6′ position, which is much larger than a hydroxy group in terms of the substituent size. The rotation barrier caused by the C-6′ sugar unit is thus sufficiently high to prevent the axial bond transition between C-1 and C-1′, which could keep **9**−**11** to exist as stable forms of atropisomers at room temperature. The stability of **9**−**11** was analyzed by treating them at different temperatures. These compounds are much more stable in comparison with compounds **1** and **2**. When heated in a solution at a temperature up to 97 °C, none of **9**−**11** showed signs of diastereoisomerization conversion to their corresponding atropisomers (Figure 6). The high stability of **9**−**11** could explain the low yields of their atropisomers in nature. In fact, we did not isolated their atropisomers from the MeOH extract of *J. procumbens*.

The CD spectral data of compounds **9**−**11** showed them as optically active compounds. Because the proximity of their β-D-glucose moiety at C-6′ to the C-1 and C-1′ chiral axial bond could significantly modify the dihedral angle between the benzene ring and the naphthalene ring, the model compound (1′***P***)-**9** that contains a sugar moiety was thus able to be introduced for the ECD calculation. The TD-DFT calculations of (1′***P***)-**9** were performed with M06-2X/def2TZVP, ωB97X-D/def2TZVP, and CAM-B3LYP/def2TZVP to ensure the accuracy of the calculations.[34] The calculated ECD spectral curves were all consistent with the experimental CD spectra of compounds **9**−**11** (Figure 7). Thus, the configurations of **9**−**11** are all determined as 1′***P*** (i.e., ***R***).

Total Synthesis of Justatropmers Atropisomers 1 and 2 and Congeners. To further confirm the ***P***- and ***M***-configurations of the isolated stable atropisomers, we designed the total synthesis of one pair of the isolated atropisomers. We selected justatropmers A (**1**) and B (**2**) for the synthetic study.

Starting from the commercially available sesamol (**13**) and 6-bromoveratraldehyde prepared from the commercially available veratraldehyde,[6] the ANL aglycone 6′-benzyloxy diphyllin (**20**) was synthesized without using costly reagents (Scheme 1). By attaching the sugar unit D-apiose, **20** was converted to compounds **22a** and **22b**, which were hydrolyzed separately by removing the protection group to afford the pair of the naturally occurred atropisomers **1**and **2**, and a pair of new atropisomers (**23** and **24**), respectively. All the four synthesized atropisomers (**1**, **2**, **23** and **24**) were obtained as stable forms of pure compounds at room temperature. The synthetic justatropmers A (**1**) and B (**2**) displayed the same NMR spectral data as those of the natural ones, and their optical rotations and CD spectra were found to be almost identical with the corresponding natural compounds.

The new synthetic **23** and **24** were also the first examples of the stably existed ANL atropisomers with a sugar unit linked at α-position. Their absolute configurations were determined by comparing their CD spectral data with those of **1** and **2** (Figure 8). Compounds **23** and **24** were thus identified as (1′***P***)-4-*O*-α-D-apiofuranosyl-6′-hydroxydiphyllin and (1′***M***)-4-*O*-α-D-apiofuranosyl-6′-hydroxydiphyllin, respectively.

Antiviral Bioactivity Evaluation of Natural and Synthetic ANL Compounds. The isolated and synthetic ANL compounds including the intermediates were evaluated for their viral entry inhibitory effects (Tables 6 and 7). Significant activity discrepancy between a pair of atropisomers was observed among the four pairs of ANL atropisomers (**1**−**8**). Compounds **1**, **3**, **5**, and **7** with a 1′***P*** configuration demonstrated much more potent antiviral activity than their corresponding 1′***M*** atropisomer compounds **2**, **4**, **6**, and **8**. The biological activity data revealed the ANL atropisomers with a ***P*** configuration as more promising antiviral compound leads than those with an ***M*** configuration. This finding provided the strong evidence that the axial rotation stereochemistry should be taken

https://doi.org/10.1021/acs.joc.1c00068
J. Org. Chem. 2021, 86, 5568−5583

Table 5. Spectral Data of Justicidinosides B (9) and C (10) and Justatropmer I (11)

	^{1}H (400 MHz) and ^{13}C (100 MHz) NMR Data in CD_3OD (δ, ppm, J, Hz)								
	9			**10**			**11**		
position	δ_H (J, Hz)	δ_C, type	key HMBC correlations	δ_H (J, Hz)	δ_C, type	key HMBC correlations	δ_H (J, Hz)	δ_C, type	key HMBC correlations
1		131.01, C			136.82, C			131.58, C	
2		121.66, C			120.67, C			121.23, C	
3		125.30, C			141.21, C			125.16, C	
4		148.99, C		7.739, s	119.71, C	C-12, C-5, C-1, C-9		146.35, C	
5	7.450, s	101.68, CH	C-4, C-6, C-7, C-9	7.244, s	107.38, CH	C-4, C-6, C-7, C-9	7.645, s	101.71, CH	C-4, C-6, C-7, C-9
6		152.68, C			153.05, C			152.13, C	
7		151.45, C			151.37, C			151.30, C	
8	6.937, s	106.90, CH	C-1, C-6, C-7, C-10	6.993, s	106.61, CH	C-1, C-6, C-7, C-10	7.084, s	107.10, CH	C-1, C-6, C-7, C-10
9		126.87, C			134.81, C			128.24, C	
10		131.46, C			129.86, C			131.51, C	
11		172.52, C			173.01, C			173.32, C	
12	5.547, d, (15.1)	68.54, CH_2	C-2, C-4, C-11	5.323, d, (15.1)	69.90, CH_2	C-2, C-4, C-11	5.361, d, (15.1)	68.34, CH_2	C-2, C-4, C-11
	5.590, d, (15.1)			5.362, d, (15.1)			5.362, d, (15.1)		
6-OCH_3	3.895, s	56.25, CH_3	C-6	3.906, s	56.36, CH_3	C-6	3.988, s	56.27, CH_3	C-6
7-OCH_3	3.706, s	56.09, CH_3	C-7	3.713, s	56.13, CH_3	C-7	3.749, s	56.10, CH_3	C-7
4-OCH_3	4.094, s	59.84, CH_3	C-4						
1′		118.95, C			118.84, C			119.33, C	
2′	6.459, s	111.15, CH	C-4′, C-6′	6.527, s	110.88, CH	C-4′, C-6′	6.598, s	111.47, CH	C-4′, C-6′
3′		144.17, C			144.22, C			144.22, C	
4′		149.60, C			149.79, C			149.51, C	
5′	7.089, s	100.98, CH	C-1′, C-3′	7.096, s	100.99, CH	C-1′, C-3′	6.991, s	100.99, CH	C-1′, C-3′
6′		151.89, C			151.65, C			151.83, C	
7′	5.971, d (1.0)	102.90, CH_2	C-3′, C-4′	5.971, d (1.0)	102.96, CH_2	C-3′, C-4′	5.993, d (1.0)	102.86, CH_2	C-3′, C-4′
	6.004, d (1.0)			6.005, d (1.0)			6.022, d (1.0)		
1″	4.685, d (7.9)	103.57, CH	C-6′, C-3″, C-4″	4.711, d (7.9)	103.43, CH	C-6′, C-3″, C-4″	4.686, d (7.9)	103.49, CH	C-6′, C-3″, C-4″
2″	2.884, dd (7.9, 9.1)	74.70, CH	C-3″, C-4″, C-1‴	2.866, dd (7.9, 9.1)	74.72, CH	C-3″, C-4″, C-1‴	2.897, dd (7.9, 9.1)	74.73, CH	C-3″, C-4″, C-1‴
3″	3.263, m	77.91, CH	C-1″, C-5″	3.269, m	77.96, CH	C-1″, C-5″	3.246, m	77.96, CH	C-1″, C-5″
4″	3.172, t (9.2)	71.30, CH	C-5″, C-2″	3.151, t (9.2)	71.31, CH	C-5″, C-2″	3.176, t (9.2)	71.28, CH	C-5″, C-2″
5″	3.350, m	77.94, CH	C-6″, C-1″, C-3″	3.382, m	77.99, CH	C-6″, C-1″, C-3″	3.346, m	77.97, CH	C-6″, C-1″, C-3″
6″	3.587, dd (5.8, 12.0)	62.50, CH_2	C-5″	3.571, dd (5.8, 12.0)	62.52, CH_2	C-5″	3.593, dd (5.8, 12.0)	62.47, CH_2	C-5″
	3.793, dd (2.0, 10.5)			3.786, dd (2.0, 10.5)			3.791, dd (2.0, 10.5)		

	HR-ESI-MS, molecular formula, UV, IR data, and sugar linkages		
	9	**10**	**11**
HR-ESI-MS	m/z: 595.1472 $[M + Na]^+$ Calcd for 595.1422	m/z 543.1351 $[M + H]^+$, Calcd for 543.1497 m/z 565.1355 $[M + Na]^+$, Calcd for 565.1355	m/z 581.1305 $[M + Na]^+$, Calcd for 581.1226
MW	$C_{28}H_{28}O_{13}$	$C_{27}H_{26}O_{12}$	$C_{27}H_{26}O_{13}$
UV (MeOH)	λ_{max} (log ε): 202 (3.06), 236 (2.85), 268 (3.09), 308 (sh) (2.51), 360 (sh) (2.11) nm	λ_{max} (log ε): 202 (2.93), 222 (2.68), 261 (3.04), 305 (sh) (2.39), 358 (sh) (1.95) nm	λ_{max} (log ε): 206 (3.11), 234 (2.92), 270 (3.11), 306 (sh) (2.53), 361 (sh) (2.14) nm
IR (KBr)	ν_{max}: 3427, 2917, 1748, 1621, 1506, 1491, 1430, 1360, 1242, 1214, 1167, 1074, 1037, 933, 859, 770 cm^{-1}	ν_{max}: 3435, 2921, 1749, 1625, 1504, 1480, 1435, 1388, 1344, 1262, 1218, 1165, 1074, 1038, 933, 891 cm^{-1}	ν_{max}: 3432, 2918, 1742, 1626, 1506, 1491, 1405, 1360, 1260, 1211, 1165, 1074, 1037, 933, 859 cm^{-1}
sugar linkages	6′-*O*-β-D-glucopyranosyl	6′-*O*-β-D-glucopyranosyl	6′-*O*-β-D-glucopyranosyl
CD (MeOH)	λ ($\Delta\varepsilon$) 200 (−33.9), 210 (8.95), 218 (6.76), 228 (18.6), 244 (−2.80), 257 (−2.5), 269 (−7.7), 295 (3.06), 316 (0.81) nm	λ ($\Delta\varepsilon$): 200 (−30.2), 210 (2.74), 227 (20.23), 252 (−7.93), 261 (−5.43), 266 (−5.63), 294 (2.69), 314 (0.67) nm	λ ($\Delta\varepsilon$): 200 (−27.9), 210 (9.43), 219 (4.75), 229 (16.67), 243(−4.43), 256 (−2.82), 269 (−6.23), 293 (2.74), 316 (0.99) nm

into consideration for rational synthetic design of ANL-like compounds for antiviral drug development.

In addition, the bioassay data also revealed that the antiviral efficacy of the ANL compounds was decreased when the number of the sugar units attached at C-4 was increased. The reason for the weakened antiviral activity could be due to existence of the steric bulk of a large sugar moiety that prevented the enlarged structure of the ANL compound to interact with the active sites of the viral molecular targets.

Although the ANL ***P***-atropisomers showed better antiviral activities than their corresponding ***M***-atropisomer counterparts, compounds **9**−**11** with a ***P***-configuration did not display viral inhibitory effects at a concentration of 50 μM, indicating the large bulk of substituents at C-6′ could possess negative impact on the antiviral activity of ANL compounds.

https://doi.org/10.1021/acs.joc.1c00068
J. Org. Chem. 2021, 86, 5568−5583

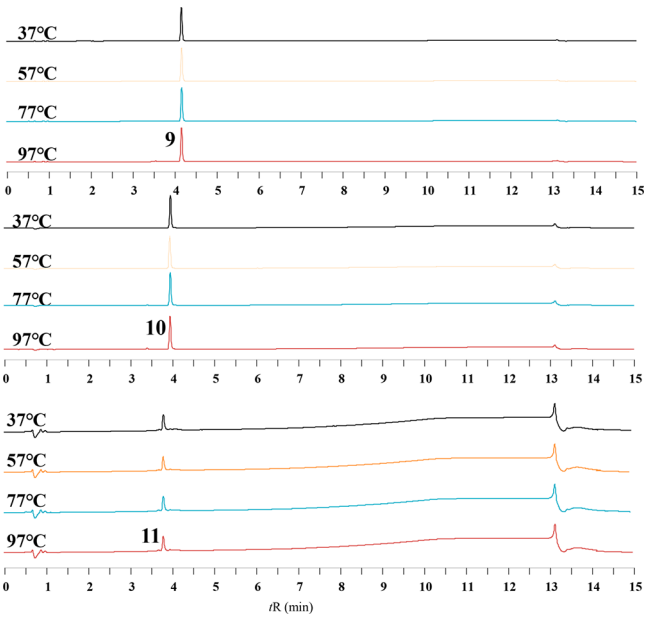

Figure 6. UHPLC analysis of the stability of compounds **9**−**11** at different temperatures.

The synthetic **1**, **2**, **23**, and **24** as well as the intermediates **15** and **19**−**21** were evaluated for their antiviral activity in comparison with diphyllin. As expected, synthetic **1** and **2** showed anti-HIV activities similar to those of the natural isolates (Table 7). The successful synthesis of **1** and **2** not only verified their atropisomer structures but also confirmed their biological activities. In the synthetic study, we further found that the α-sugar linked ANLs (**23** and **24**) showed much weaker antiviral activities than their β-sugar linked counterparts (**1** and **2**), which indicates a β-glycosidic linkage may be essential to maintain the antiviral potency of ANL compounds.

CONCLUSIONS

The discovery of the new ANL atropisomers from *Justicia* plants demonstrates remarkable ability of the nature to produce novel structurally interesting secondary metabolites with diversified chemical structures that can be an excellent source for new drug development. The isolated justatropmers A−H (**1**−**8**) as the first naturally stable atropisomer examples with axial chirality represents a milestone during the decades of the research efforts to study natural arylnaphthalene lignans. The plausible biosynthetic pathway of the atropisomers is summarized in Figure S6. The 1′***P*** configuration of the atropisomers is having the 6′-hydroxyl group placed upside the plane of the naphthalene lactone ring. The ***P***-configured ANL atropisomers showed much stronger antiviral activity than their ***M***-configured ANL counterparts, revealing the axial orientation between the biphenyls is crucial to allow an ANL compound to have specificity of binding affinity with a viral protein target. The ***P***-configuration to own stronger antiviral activity has determined the favorable direction of the stereochemistry to synthesize ANL compounds with highly potent antiviral activity.

EXPERIMENTAL SECTION

General Experimental Procedures. Optical rotations were measured with a PerkinElmer model 241 polarimeter (Maryland). IR spectra were recorded on a JASCO FT/IR-410 spectrometer, equipped with a Specac Silver Gate ATR system by applying a film on a germanium plate (Maryland). CD spectra were recorded on a JASCO J-1500 CD spectrometer (Maryland). 1D and 2D NMR spectra were recorded on a Bruker DRX-500 MHz or a Bruker DPX- 400 MHz (Rheinstetten, Germany). Chemical shifts (δ) are expressed in ppm with reference to the solvent signals [methanol-d_4 (CD_3OD): ^{1}H: 3.31 ppm, ^{13}C: 49.00 pm; dimethyl sulfoxide-d_6 (DMSO-d_6): ^{1}H: 2.50 ppm, ^{13}C: 39.52 pm], and coupling constants (J) are reported in hertz. All NMR experiments were obtained by using standard pulse sequences supplied by the vendor. Column chromatography was carried out on silica gel (230−400 mesh, Natland International Corp., North Carolina). Reversed-phase flash chromatography was accomplished with RP-18 silica gel (40−63 mm, EM Science, New Jersey), and reversed-phase preparative HPLC was carried out on a Agilent 1200 series Delivery System pump, equipped with a Agilent 1200 series photodiode detector (California), and a YMC-Pack ODS-A C18 column (120 Å, 5 μm, 250 × 20 mm^2, Tokyo, Japan) or a Alltima C18 column (120 Å, 5 μm, 250 × 10 mm^2, Chicago, IL). Thin-layer chromatography was performed on EMD glass-backed plates coated with 0.25 mm layers of Silica gel 60 F_{254} (Darmstadt, Germany). HRTOFMS spectra were recorded on an Agilent 6540 Q-TOF (California) or an Agilent 6460 Triple Quadrupole (California) or a Bruker Q-TOF mass spectrometer (Rheinstetten, Germany). Structural assignments were made with additional information from gCOSY, gHSQC, gHMBC, and gNOESY experiments.

Plant Materials. The aerial parts of *Justicia procumbens* were collected in Ningde city of Fujian Province, China, in July of 2013. The identification was conducted by Professor Hubiao Chen, School of Chinese Medicine, Hong Kong Baptist University. A voucher specimen (SHA00026) is available for inspection at the Quality

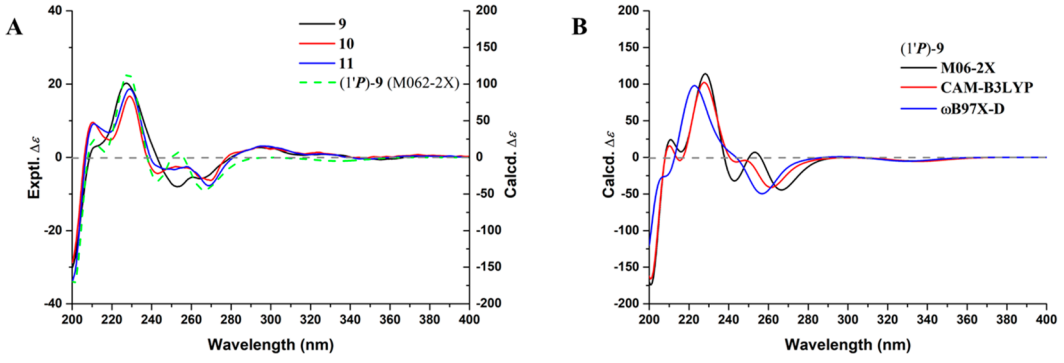

Figure 7. Determination of the configurations of **9**−**11** by comparison of their experimental CD spectra with the calculated ECD of the model compound (1′***P***)-**9**. (A) The experimental CD spectra for **9**−**11** and the calculated ECD for (1′***P***)-**9** in M06-2X/def2TZVP (shift = +14 nm). (B) The ECD spectra of (1′***P***)-**9** in M06-2X/def2TZVP (shift = +14 nm), CAM-B3LYP/def2TZVP (shift = +13 nm) and ωB97X-D/def2TZVP (shift = +11 nm).

https://doi.org/10.1021/acs.joc.1c00068
J. Org. Chem. 2021, 86, 5568−5583

Scheme 1. Synthesis of 1, 2, and Their Congeners[a]

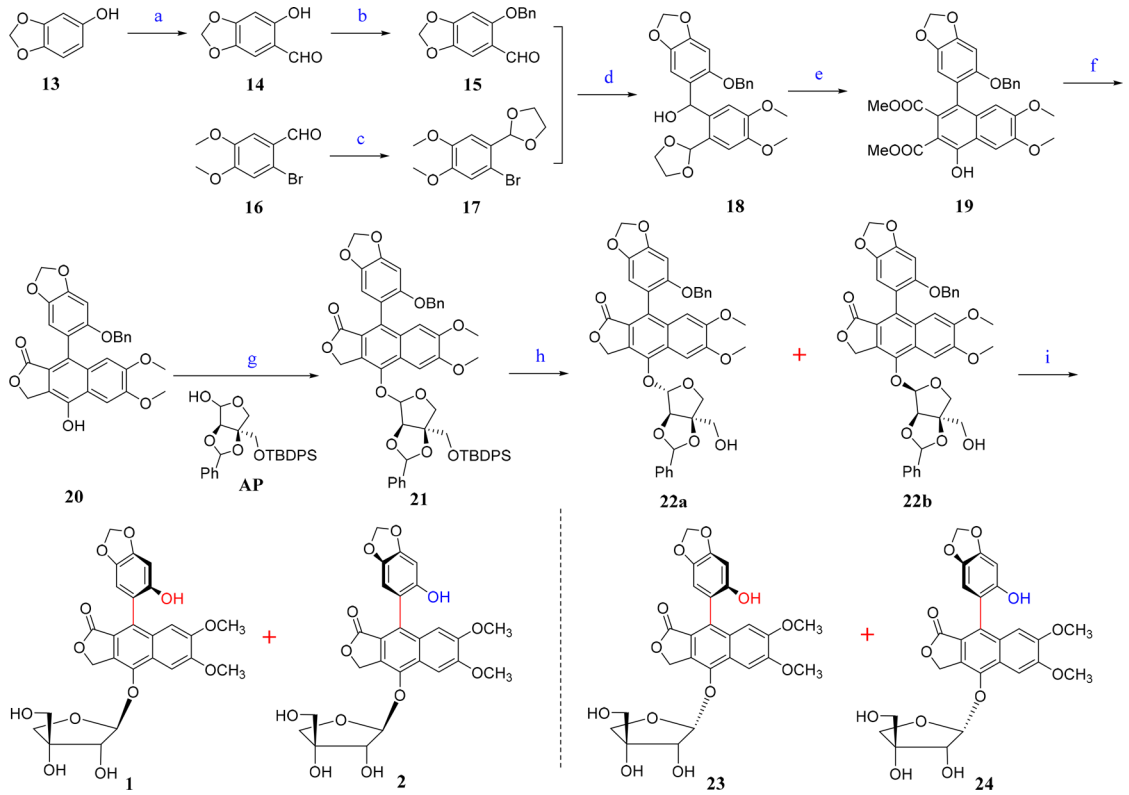

[a]Reagents and conditions: (a) (HCHO)n (paraformaldehyde), anhydrous $MgCl_2$, Et_3N (trimethylamine), THF, 80 °C, 8 h, 91%; (b) BnBr (benzyl bromide), Cs_2CO_3, THF, 80 °C, 5 h, 91%; (c) ethylene glycol, TsOH·H_2O (*p*-toluenesulfonic acid monohydrate), toluene, refluxe, 8 h, 86%; (d) *n*-BuLi (*n*-butyllithium), THF, −78 °C, 3 h, 96%; (e) DMADC (dimethyl acetylenedicarboxylate), AcOH (acetic acid), CH_2Cl_2 (dichloromethane), 43 °C, 1 h, 56%; (f) (1) $NaBH_4$, THF, reflux, 3 h, (2) 3 M HCl, 60%; (g) **AP** [(3a*R*,6a*S*)-6a-(((*tert*-butyldiphenylsilyl)oxy)methyl)-2,2-dimethyltetrahydrofuro[3,4-*d*][1,3]dioxol-4-ol], PPh_3 (triphenylphosphine), DIAD (diisopropyl azodicarboxylate), THF, 0 °C, 5 h, 96%; (h) TBAF (tetrabutylammonium fluoride), THF, rt (room temperature), 1 h, 36% (**22a**), 61% (**22b**); (i) $Pb(OH)_2$, H_2, THF/MeOH(1:3), rt, 12 h; 42% (**1**),44% (**2**), 43% (**23**), 44% (**24**).

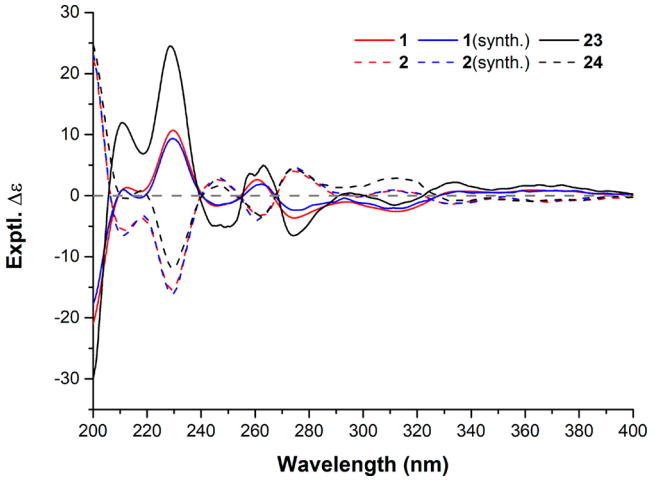

Figure 8. Experimental CD spectra for **1** and **2**, synthesized **1** and **2** and their isomerized apioside congeners **23** and **24**.

Table 6. Antiviral Activities of the Natural ANLs (1−11) against VSV-Pseudotyped HIV-1

name	inhibitory rate (%)[a]	EC_{50} (μM)	CC_{50} (μM)	SI = CC_{50}/EC_{50}
1		2.7 ± 0.6	46.8 ± 6.3	17.3
2		48.6 ± 8.6	>50	
3		5.4 ± 0.6	23.5 ± 4.8	4.3
4		23.1 ± 3.7	>50	
5		15.7 ± 2.3	>50	
6	28.8		>50	
7		14.7 ± 3.1	>50	
8	39.5		>50	
9	4.2		>50	
10	12.1		>50	
11	10.6		>50	
Diphyllin		0.17 ± 0.03	2.46 ± 0.75	14.6

[a]Inhibitory rate at 25 μM.

Research Laboratory/Photochemistry Laboratory, School of Chinese Medicine, Hong Kong Baptist University.

Extraction and Isolation. The dried and powdered aerial parts of *J. procumbens* (18.0 kg) were extracted with MeOH (60 L × 4) at room temperature (12 h each time) and filtered to yield a filtrate. Concentration of the filtrate under vacuum gave a brown residue, which was dissolved in H_2O, followed by successive partitions of PE (petroleum ether) (4 × 5 L), EtOAc (ethyl acetate) (4 × 5 L), and *n*-BuOH (*n*-butanol) (4 × 5 L) to afford PE-soluble, EtOAc-soluble, *n*-BuOH-soluble, and H_2O-soluble extracts after dryness *in vacuo*. The EtOAc soluble fraction (154.0 g), which demonstrated the most potent anti-HIV-1 activity among the four portions, was chromatographed over a silica gel column (100−230 mesh; 10 × 150 cm), eluting with gradient PE/Me_2CO (acetone) (8:1, 10 L; 4:1, 10 L; 3:1, 10 L; 1:1, 10 L), followed by CH_2Cl_2/MeOH (8:2, 10 L; 7:3, 10 L; 0:10 10 L) solutions to yield 140 fractions, and then combined into 14

https://doi.org/10.1021/acs.joc.1c00068
J. Org. Chem. 2021, 86, 5568−5583

Table 7. Antiviral Activities of the Synthetic Compounds against VSV-Pseudotyped HIV-1

name	inhibitory rate[a] (%)	EC_{50} (μM)	CC_{50} (μM)	SI = CC_{50}/EC_{50}
1 (synth)		3.2 ± 0.2	>50	13.6
2 (synth)		40.6 ± 11.4	>50	
15	15.6		>50	
19	29.2		>50	
20	38.5		28.9	
21	−5.2		>50	
23	29.4		>50	
24	18.6		>50	
diphyllin		0.17 ± 0.03	2.46 ± 0.75	14.6

[a]Inhibitory rate at 25 μM.

fractions (F1−14) based on the UV absorption and TLC chromatography. Fractions F10−F12 showed the most potent anti-HIV-1 activity and were further chromatographed over a MCI column chromatography (CC) and eluted with aqueous MeOH (0, 20%, 40%, 60%, and 80%) to afford 16 fractions (FA-FP). Fraction FK was subjected to a semipreparative HPLC separation (YMC-Pack ODS-A C18 column, solvent system MeCN (acetonitrile)/H_2O 35:65, flow: 4 mL/min) to yield 11 fractions (FK1-FK11). FK11 was subjected to a semipreparative HPLC separation and eluted with MeCN/H_2O (30%) (Alltima C18 column, flow rate at 2 mL/min, UV detection at λ = 210 nm) to give **9** (75.3 mg, t_R = 40.5 min). FK9 and FK10 were pooled and subjected to a semipreparative HPLC separation with MeCN/H_2O (29%) (Alltima C18 column, flow rate at 2 mL/min, UV detection at λ= 210 nm) to afford **1** (85.8 mg, t_R = 35.3 min) and **2** (90.2 mg, t_R = 43.5 min). FK8 was subjected to a silica gel column separation by elution with $CHCl_3$/MeOH (15:1) to give **10** (80.8 mg). FK7 and FK6 were pooled and subjected to a semipreparative HPLC separation with MeCN/H_2O (28%) (Alltima C18 column, flow rate at 2 mL/min, UV detection at λ= 210 nm) to give **3** (5.8 mg, t_R = 27.2 min), **4** (7.2 mg, t_R = 36.4 min), and **11** (5.2 mg, t_R = 34.9 min). FK5 was separated by a semipreparative HPLC separation, and eluted with MeCN/H_2O (27.5%) (Alltima C18 column, flow rate at 2 mL/min, UV detection at λ= 210 nm) to give **5** (7.8 mg, t_R = 26.5 min) and **6** (13.7 mg, t_R = 35.2 min). FK4 was subjected to a semipreparative HPLC separation with MeCN/H_2O (27%) (Alltima C18 column, flow rate at 2 mL/min, UV detection at λ = 210 nm) to afford **7** (9.3 mg, t_R = 24.9 min) and **8** (13.7 mg, t_R = 34.2 min). Fraction FL was subjected to a silica gel column separation by elution with $CHCl_3$/MeOH (15:1) to yield **12** (7.2 mg).

*Justatropmer A (**1**).* White power; $[\alpha]_D^{20}$ −83.3 (*c* 0.05, MeOH); the spectral data of UV, IR, CD, HRMS, and ^1H and ^{13}C NMR and the key HMBC correlation data: Table 1.

*Justatropmer B (**2**).* White power; $[\alpha]_D^{20}$ −77.9 (*c* 0.05, MeOH); the spectral data of UV, IR, CD, HRMS, and ^1H and ^{13}C NMR and the key HMBC correlation data: Table 1.

*Justatropmer C (**3**).* Colorless power; $[\alpha]_D^{20}$ −39.1 (*c* 0.05, MeOH); the spectral data of UV, IR, CD, HRMS, and ^1H and ^{13}C NMR and the key HMBC correlation data: Table 2.

*Justatropmer D (**4**).* White power; $[\alpha]_D^{20}$ −37.5 (*c* 0.05, MeOH); the spectral data of UV, IR, CD, HRMS, and ^1H and ^{13}C NMR and the key HMBC correlation data: Table 2.

*Justatropmer E (**5**).* White power; $[\alpha]_D^{20}$ −39.6 (*c* 0.05, MeOH); the spectral data of UV, IR, CD, HRMS, and ^1H and ^{13}C NMR and the key HMBC correlation data: Table 3.

*Justatropmer F (**6**).* Colorless power; $[\alpha]_D^{20}$ −50.2 (*c* 0.05, MeOH); the spectral data of UV, IR, CD, HRMS, and ^1H and ^{13}C NMR and the key HMBC correlation data: Table 3.

*Justatropmer G (**7**).* White power; $[\alpha]_D^{20}$ −43.7 (*c* 0.05, MeOH); the spectral data of UV, IR, CD, HRMS, and ^1H and ^{13}C NMR and the key HMBC correlation data: Table 4.

*Justatropmer H (**8**).* White power; $[\alpha]_D^{20}$ (*c* 0.05, MeOH); the spectral data of UV, IR, CD, HRMS, and ^1H and ^{13}C NMR and the key HMBC correlation data: Table 4.

*Justicidinoside B (**9**).* White power; $[\alpha]_D^{20}$ −14.8 (*c* 0.05, MeOH); the spectral data of UV, IR, CD, HRMS, and ^1H and ^{13}C NMR and the key HMBC correlation data: Table 5.

*Justicidinoside C (**10**).* White power; $[\alpha]_D^{20}$ −18.5 (*c* 0.05, MeOH); the spectral data of UV, IR, CD, HRMS, and ^1H and ^{13}C NMR and the key HMBC correlation data: Table 5.

*Justatropmer I (**11**).* White power; $[\alpha]_D^{20}$ −14.8 (*c* 0.05, MeOH); the spectral data of UV, IR, CD, HRMS, and ^1H and ^{13}C NMR and the key HMBC correlation data: Table 5.

Acid Hydrolysis of 1−11. Compound **1** (2.0 mg) was treated with 2 M trifluoroacetic acid (TFA, 2 mL) for 3 h in a screw-cap vial at room temperature. The hydrolysate was centrifuged (10000*g*, 5 min), and the precipitate was suspended in water (3 mL) and was partitioned with $CHCl_3$ (3 mL, × 2). The CH_2Cl_2 extraction was evaporated to dryness under vacuum to afforded the aglycone of **1**. The supernatant aqueous layer containing the monosaccharide was evaporated to dryness under vacuum to remove TFA. Following the same reaction protocol, compounds **2**−**11** produced their corresponding aglycones and monosaccharides. The obtained monosaccharides were subjected to TLC analysis in comparison with the authentic sugar samples D-apiose, D-glucose, and D-xylose (developing solvent system: EtOAc/i-PrOH/MeOH/H_2O = 100:60:30:30, visualization with EtOH (ethanol)−5% H_2SO_4 spraying).

Atropisomeric Stability Analysis of Compounds 1, 2, and 9−11 Tested at Different Temperatures. A compound (**1**, **2**, **9**, **10**, or **11**) (0.5 mg) was dissolved in DMF/H_2O (0.2 mL/0.6 mL) in a screw-cap vial and heated at 37, 57, 77, and 97 °C for 1 h, respectively. After the solution was cooled to room temperature, 20 μL of the heated reaction product was taken and dissolved in MeOH (1 mL), which was analyzed on a UHPLC system (Agilent Technologies 1290 Infinity, CA). The chromatographic separation was performed with a Waters ACQUITY BEH C18 (1.7 μm, 2.1 mm × 100 mm) column and a guard column (2.1 mm × 5 mm). The mobile phase consisted of (A) water and (B) MeCN. The elution condition was optimized as follows: 0−6 min 5−75% B in A; 6−9 min 75−100% B in A; 9−12 min 100−5% B in A; 12−15 min 5% B in A. The flow rate was 0.4 mL/min. The column was maintained at 25 °C. UV detection was set at λ= 254 nm. The injection volume was 2 μL.

X-ray Crystallographic Analysis of 5. The details are included in Figure S5 and Table S7. The crystallographic data for the structure of **5** have been deposited with the Cambridge Crystallographic Data Centre (deposition no. CCDC 1974784). Copies of the data can be obtained free of charge from the CCDC via www.ccdc.cam.ac.uk.

Chemical Synthesis of Justatropmers A (1) and B (2) and Their Isomerized Glycoside Congeners (23 and 24). A schematic illustration for the synthesis of justatropmers A (**1**) and B (**2**) is summarized in Scheme 1. All starting materials and reagents were commercially available. All intermediates and reaction products were purified by silica gel column chromatography, and their structures were analyzed according to the MS and NMR data.

*6-(Hydroxy)benzo[d][1,3]dioxole-5-carbaldehyde (**14**).* To a solution of sesamol (commercially purchased, 1.40 g, 10.14 mmol), anhydrous $MgCl_2$ (1.50 g, 15.78 mmol), and Et_3N (5 mL) in anhydrous THF (50 mL) was added parafomaldehyde (1.50g, 49.95 mmol), and the mixture was refluxed at 80 °C in an oil bath for 10 h. After the mixture was cooled to rt, the reaction was quenched with 3 M HCl (1.5 mL). The mixture was extracted with EtOAc (3 × 50 mL), which was combined and further washed with brine, dried over anhydrous Na_2SO_4, filtered, and concentrated. The residue was purified by column chromatography on a silica gel column by elution with PE/EtOAc 10:1 to afford compound **14**[35] as a light yellow solid (1.53 g, 90.9%): HRMS (ESI) *m*/*z*: $[M + H]^+$ calcd for $C_8H_7O_4$, 167.0339; found, 167.0340.

*6-(Benzyloxy)benzo[d][1,3]dioxole-5-carbaldehyde (**15**).* To a solution of **14** (0.53 g, 3.16 mmol) and Cs_2CO_3 (2.01 g, 6.14 mmol) in anhydrous DMF (15 mL) was added BnBr (1.00g, 0.72 mL, 5.85 mmol) under argon, and the mixture was refluxed in an oil bath

https://doi.org/10.1021/acs.joc.1c00068
J. Org. Chem. 2021, 86, 5568−5583

for 5 h at 80 °C. After the mixture was cooled to room temperature, the reaction was quenched with 3 M HCl (1.5 mL) and extracted with EtOAc (3 × 50 mL). The combined organic extracts were washed with brine, dried over anhydrous Na_2SO_4, filtered, and concentrated. The residue was purified by column chromatography on silica gel (PE/EtOAc, 8:1) to afford compound **15**[35] as a light yellow solid (0.74 g, 91.3%): HRMS (ESI) *m/z*: $[M + H]^+$ calcd for $C_{15}H_{13}O_4$, 257.0808; found, 257.0826.

*2-(2-Bromo-4,5-dimethoxyphenyl)-1,3-dioxolane (**17**).* To a solution of 6-bromoveratraldehyde (**16**) (commercially purchased, 3.48 g, 14.20 mmol) in toluene (50 mL) were added ethylene glycol (1.76 g, 28.38 mmol) and TsOH·H_2O (0.27 g, 14.21 mmol). A Dean−Stark apparatus filled with toluene was fitted to the round-bottom flask, and the reaction was refluxed in an oil bath for 8 h at 135 °C. After cooling, the reaction was quenched with Et_3N (0.5 mL), and the mixture was washed with water (2 × 20 mL) and brine (20 mL). After the organic solvent was removed under vacuum, the obtained mixture was triturated with EtOH. The obtained solid was dried under vacuum to provide **17**[35] as a white solid (3.53 g, 85.8%); HRMS (ESI) *m/z*: $[M + H]^+$ calcd for $C_{11}H_{14}BrO_4$, 289.0070; found, 289.0098.

*(2-(1,3-Dioxolan-2-yl)-4,5-dimethoxyphenyl)-(6-benzyloxy)-benzo[d][1,3]dioxol-5-yl)methanol (**18**).* Compound **17** (794.90 mg, 2.76 mmol) was dissolved in dry THF (10 mL) under nitrogen and cooled to −78 °C over 20 min. To the solution was added *n*-BuLi (2.5 M in hexanes, 1 mL, 2.50 mmol) dropwisely. The mixture was stirred for another 20 min, followed by the addition of the THF (3 mL) solution of compound **15** (627.42 mg, 2.45 mmol) dropwisely. After being stirred for 3 h, the mixture was gradually warmed to rt, followed by the addition of H_2O (10 mL). The reaction mixture was then extracted with EtOAc (2 × 50 mL). The combined organic extracts were washed with brine, dried over anhydrous Na_2SO_4, filtered, and concentrated to afford **18**[35] as a white solid (1.10 g, 96.3%): HRMS (ESI) *m/z*: $[M + H]^+$ calcd for $C_{26}H_{27}O_8$, 467.1700; found, 467.1637. Since compound **18** was unstable at room temperature, the compound was immediately dissolved in CH_2Cl_2 for the next step of reaction after its HRMS was measured.

*Diethyl 1-(6-(Benzyloxy)benzol[d][1,3]dioxol-5-yl)-4-hydroxy-6,7-dimethoxynaphthalene-2,3-dicarboxylate (**19**).* Compound **18** (1.10 g, 2.36 mmol), DMADC (433.73 mg, 2.97 mmol), and AcOH (1 mL) were added in CH_2Cl_2 (1.5 mL), and the mixture was heated in an oil bath at 80 °C for 1 h. After workup, the mixture was gradually warmed to rt followed by addition of H_2O (10 mL). The mixture was then extracted with EtOAc (2 × 50 mL). The combined organic solutions were washed with brine, dried over anhydrous Na_2SO_4, filtered, and concentrated to give a light green solid, which was purified by column chromatography on silica gel (PE/EtOAc 4:1) to give the desired product **19**[35] as a light green solid (550.53 mg, 42.7%): HRMS (ESI) *m/z*: $[M + H]^+$ calcd for $C_{30}H_{27}O_{10}$, 547.1599; found, 547.1607; ^1H NMR (DMSO-d_6, 400 MHz) δ_H 11.76 (1H, s), 8.31 (1H, s), 7.64 (1H, s), 7.11−7.17 (3H, m), 6.92−6.94 (2H, m), 6.65 (1H, s), 6.64 (1H, s), 6.04 (1H, d, *J* = 1.0 Hz), 6.05 (1H, d, *J* = 1.0 Hz), 4.93 (2H, s), 3.93 (3H, s), 3.88 (3H, s), 3.60 (3H, s), 3.53 (3H, s).

*6′-Benzyloxydiphyllin (**20**).* To a solution of compound **19** (191.15 mg, 0.35 mmol) in dry THF (4 mL) was added $NaBH_4$ (66.20 mg, 1.75 mmol), and the reaction was allowed to reflux in an oil bath for 4 h at 80 °C. After the solution was cooled to rt, HCl (3 mol/L) was added to adjust the pH value to 2−3 (approximate 1.5 mL), and the mixture was stirred for additional 1 h. The reaction mixture was extracted with EtOAc (3 × 50 mL). The combined organic extracts were washed with brine, dried over anhydrous Na_2SO_4, filtered, and concentrated and further purified by a silica gel column (PE/EtOAc 1:1) to give the desired product **20**[35] as a white solid (102.10 mg, 60.0%); HRMS (ESI) *m/z*: $[M + H]^+$ calcd for $C_{28}H_{23}O_8$, 487.1387; found, 487.1355; ^1H NMR (DMSO-d_6, 400 MHz) δ_H 10.37 (1H, s, 4-OH), 7.62 (1H, s, H-5), 6.95 (1H, s, H-8), 7.11−7.18 (3H, m, H-11′-13′), 6.88−6.91 (2H, m, H-10′, 14′), 6.85 (1H, s, H-2′), 6.74 (1H, s, H-5′), 6.06 (1H, d, *J* = 1.0 Hz, H-7′), 6.07 (1H, d, *J* = 1.0 Hz, H-7′), 5.35 (2H, s, H-8′), 4.86 (1H, d, *J* = 12.3 Hz, H-12), 4.92 (1H, d, *J* = 12.3 Hz, H-12), 3.94 (3H, s, 6-OCH_3), 3.61 (3H, s, 7-OCH_3).

*1-(3aR,6aS)-6a-(((tert-Butyldiphenylsilyl)oxy)methyl)-2-phenyltetrahydrofuro [3,4-d][1,3]dioxol-4-ol-6′-benzyloxydiphyllin (**21**).* An oven-dried 25 mL flask charged with **20** (102.10 mg, 0.21 mmol), **AP** (142.86 mg, 0.30 mmol), and PPh3 (104.91 mg, 0.40 mmol) in THF (8 mL) was added DIAD (80.88 mg, 0.40 mmol) at 0 °C under nitrogen protection. After the reaction was stirred at rt for 2 h, the reaction mixture was extracted with EtOAc (3 × 50 mL). The combined organic extracts were washed with brine, dried over anhydrous Na_2SO_4, filtered, and concentrated and further purified by a silica gel column (PE/EtOAc 2:3) to give the desired product **21** as a light yellow solid (190.20 mg, 95.9%, mixture): HRMS (ESI) *m/z*: $[M + H]^+$ calcd for $C_{56}H_{53}O_{12}Si$, 945.3301; found, 945.2910; ^1H NMR ($CDCl_3$, 400 MHz) δ_H 7.43 (1H, s, H-5), 6.98 (1H, s, H-8), 7.13−7.17 (3H, m, H-11′-13′), 6.93−6.99 (2H, m, H-10′, 14′), 6.70 (1H, s, H-5′), 6.72 (1H, s, H-2′), 5.99 (1H, d, *J* = 1.3 Hz, H-7′), 6.04 (1H, d, *J* = 1.3 Hz, H-7′), 5.51 (2H, s, H-8′), 4.23 (1H, d, *J* = 11.0 Hz, H-12), 4.43 (1H, d, *J* = 11.0 Hz, H-12), 3.42 (3H, s, 6-OCH_3), 3.76 (3H, s, 7-OCH_3). 5.42(1H, s, H-1″), 4.04 (1H, d, *J* = 12.0 Hz, H-4″), 4.15(1H, d, *J* = 12.0 Hz, H-4″), 4.14 (1H, s, H-2″), 4.90 (2H, s, H-6″), 6.46 (1H, s, H-5″), 7.40−7.42 (3H, m, H-9″-11″), 7.51−7.53 (2H, m, H-8″, H-12″), 7.42−7.47 (4H, m, H-2‴, H-6‴), 7.70−7.78 (6H, m, H-3‴-5‴), 1.14−1.15 (9H,s, H-8‴-10‴); $^{13}C\{^1H\}$ NMR (100 MHz, $CDCl_3$) δ 137.57, 137.82 (s, C-1), 120.30, 120.28 (s, C-2), 130.70, 130.72 (s, C-3), 145.88, 145.76 (s, C-4), 101.70, 101.75 (d, C-5), 151.73, 151.75 (s, C-6), 151.79, 151.84 (s, C-7), 105.81, 105.84 (d, C-8), 130.01 (s, C-9), 130.17, 130.25 (s, C-10), 167.89, 170.07, 170.05 (s, C-11), 67.28 (t, C-12), 55.89 (q, OCH_3-6), 55.70 (q, OCH_3-7), 116.85, 116.83 (s, C-1′), 97.55, 97.59 (d, C-2′), 141.82, 141.83 (s, C-3′), 148.46, 148.53 (s, C-4′), 111.19, 111.16 (d, C-5′), 150.31, 150.36 (s, C-6′), 101.60 (t, C-7′), 71.87, 71.89 (t, C-8′), 137.31, 137.27 (s, C-9′), 127.59, 127.62 (d, C-10′, 14′), 128.31, 128.33 (d, C-11′, 13′), 126.98, 127.00 (d, C-12′), 107.17 (d, C-1″), 82.90 (d, C-2″), 91.63 (s, C-3″), 72.18, 72.14 (t, C-4″), 104.61, 104.65 (d, C-5″), 65.42, 65.45 (t, C-6″), 136.73, 136.72 (s, C-7″), 127.87, 127.88 (d, C-8″, 12″), 128.59, 128.64 (d, C-9″, 11″), 127.03, 127.05 (d, C-10″), 135.70 (s, C-1‴), 135.81 (d, C-2‴, C-6‴), 128.08 (d, C-3‴-5‴), 30.48 (s, C-7‴), 26.98 (q, C-8‴-10‴).

To a solution of compound **21** (100.10 mg, 0.10 mmol) in THF (4 mL) was added TBAF (0.8 mL, 1 M in THF/H_2O, 95/5). The mixture was stirred at rt for 1 h. TLC showed the reaction was complete, and two new spots with higher polarity were formed. The mixture was concentrated in vacuo to give an oil, which was separated by a silica gel column (PE/EtOAc 1:1) to afford **22a** (white solid, 25.33 mg, 35.8%) and **22b** (white solid, 45.75 mg, 61.1%).

*1-(3aR,4R,6aR)-6a-(Hydroxymethyl)-2-phenyltetrahydrofuro-[3,4-d][1,3]dioxol-4-yl)oxy)-6′-benzyloxydiphyllin (**22a**).* HRMS (ESI) *m/z*: $[M + H]^+$ calcd for $C_{40}H_{35}O_{12}$, 707.2123; found, 707.1945. ^1H NMR ($CDCl_3$, 400 MHz) δ_H 7.46 (1H, s, H-5), 7.01 (1H, s, H-8), 7.13−7.16 (3H, m, H-11′-13′), 6.92−6.95 (2H, m, H-10′, 14′), 6.68 (1H, s, H-5′), 6.70 (1H, s, H-2′), 5.98 (1H, d, *J* = 1.3 Hz, H-7′), 6.03 (1H, d, *J* = 1.3 Hz, H-7′), 5.48 (2H, s, H-8′), 4.26 (1H, d, *J* = 11.0 Hz, H-12), 4.35 (1H, d, *J* = 11.0 Hz, H-12), 4.06 (3H, s, 6-OCH_3), 3.77 (3H, s, 7-OCH_3), 5.83 (1H, s, H-1″), 4.13 (1H, d, *J* = 12.0 Hz, H-4″), 4.17(1H, d, *J* = 12.0 Hz, H-4″), 5.06 (1H, s, H-2″), 4.87 (2H, s, H-6″), 6.08 (1H, s, H-5″), 7.40−7.42 (3H, m, H-9″-11″), 7.52−7.55 (2H, m, H-8″, H-212″); $^{13}C\{^1H\}$ NMR (100 MHz, $CDCl_3$) δ 132.43 (s, C-1), 120.37 (s, C-2), 130.35 (s, C-3), 143.89 (s, C-4), 100.21 (d, C-5), 151.93 (s, C-6), 151.81 (s, C-7), 107.08 (d, C-8), 130.95 (s, C-9), 127.98 (s, C-10), 169.81 (s, C-11), 67.22 (t, C-12), 56.15 (q, OCH_3-6), 55.95 (q, OCH_3-7), 116.73 (s, C-1′), 97.62 (d, C-2′), 141.81 (s, C-3′), 148.53 (s, C-4′), 110.75 (d, C-5′), 150.38 (s, C-6′), 101.64 (t, C-7′), 71.90 (t, C-8′), 135.88 (s, C-9′), 127.02 (d, C-10′, 14′), 128.35 (d, C-11′, 13′), 126.42 (d, C-12′), 108.16 (d, C-1″), 87.34 (d, C-2″), 92.42 (s, C-3″), 74.69 (t, C-4″), 106.41 (d, C-5″), 63.55 (t, C-6″), 137.25 (s, C-7″), 127.13 (d, C-8″, 12″), 128.72 (d, C-9″, 11″), 127.61, 127.65 (d, C-10″).

*1-(3aR,4S,6aR)-6a-(Hydroxymethyl)-2-phenyltetra-hydrofuro-[3,4-d][1,3]dioxol-4-yl)oxy)-6′-benzyloxydiphyllin (**22b**).* HRMS (ESI) *m/z*: $[M + H]^+$ calcd for $C_{40}H_{35}O_{12}$, 707.2123; found, 707.1943; ^1H NMR ($CDCl_3$, 400 MHz) δ_H 7.72 (1H, s, H-5), 6.96

https://doi.org/10.1021/acs.joc.1c00068
J. Org. Chem. 2021, 86, 5568−5583

(1H, s, H-8), 7.12−7.16 (3H, m, H-11′-13′), 6.92−6.95 (2H, m, H-10′, 14′), 6.67 (1H, s, H-5′), 6.70 (1H, s, H-2′), 5.97 (1H, d, J = 1.3 Hz, H-7′), 6.02 (1H, d, J = 1.3 Hz, H-7′), 5.49 (2H, s, H-8′), 5.54 (1H, d, J = 11.0 Hz, H-12), 5.46 (1H, d, J = 11.0 Hz, H-12), 3.40 (3H, s, 6-OCH_3), 3.76 (3H, s, 7-OCH_3). 5.49 (1H, d, J = 4.3 Hz, H-1″), 4.83 (1H, d, J = 4.3 Hz, H-1″), 3.98 (1H, d, J = 11.7 Hz, H-4″), 4.04 (1H, d, J = 11.7 Hz, H-4″), 4.87 (2H, s, H-6″), 6.41 (1H, s, H-5″), 7.33−7.39 (3H, m, H-9″-11″), 7.74−7.76 (2H, m, H-8″, H-12″); $^{13}C\{^1H\}$ NMR (100 MHz, $CDCl_3$) δ 132.70, 132.65 (s, C-1), 120.24, 120.27 (s, C-2), 130.79, 130.61 (s, C-3), 145.72, 145.84 (s, C-4), 101.60, 101.62 (d, C-5), 151.78, 151.82 (s, C-6), 151.72, 151.77 (s, C-7), 105.80, 105.84 (d, C-8), 131.02 (s, C-9), 130.40 (s, C-10), 170.19, 171.34 (s, C-11), 67.38, 67,42 (t, C-12), 56.66, 56.77 (q, OCH_3-6), 55.88 (q, OCH_3-7), 116.74 (s, C-1′), 97.49, 97.54 (d, C-2′), 141.81, 141.81 (s, C-3′), 148.47 (s, C-4′), 110.72, 110.76 (d, C-5′), 150.37, 150.37 (s, C-6′), 101.62, 101.67 (t, C-7′), 71.82, 71.85 (t, C-8′), 135.25, 135.22 (s, C-9′), 127.60 (d, C-10′, 14′), 128.30, 128.32 (d, C-11′, 13′), 127.00, 127.02 (d, C-12′), 104.48 (d, C-1″), 82.76 (d, C-2″), 91.51 (s, C-3″), 72.14, 72.13 (t, C-4″), 104.32 (d, C-5″), 63.92 (t, C-6″), 136.40 (s, C-7″), 127.83, 127.84 (d, C-8″, 12″), 128.62 (d, C-9″, 11″), 127.02 (d, C-10″).

To a solution of **22a** (25.13 mg, 0.04 mmol) in the mixed solvents of THF/MeOH (1:3, 4 mL) was added $Pd(OH)_2$ on carbon (4 mg, 20%). The reaction was degassed 3 times with H_2 and stirred for 6 h under H_2 balloon. TLC showed the **22a** disappeared, and two new spots with higher polarity were formed. The mixture was purified by a silica gel column (PE/EtOAc 1:1) to provide justatropmers A (**1**) (white powder, 7.80 mg, 42.2%) and B (**2**) (white powder, 8.10 mg, 43.8%).

*Justatropmer A (**1**) (Synthetic).* HRMS (ESI) m/z: $[M + H]^+$ calcd for $C_{26}H_{25}O_{12}$, 529.1346; found, 529.1339; ^1H NMR (CD_3OD, 400 MHz) δ_H 7.701 (1H, s, H-5), 7.075 (1H, s, H-8), 6.567 (1H, s, H-2′), 6.543 (1H, s, H-5′), 5.946 (1H, d, J = 1.0 Hz, H-7′), 5.968 (1H, d, J = 1.0 Hz, H-7′), 5.498 (1H, d, J = 14.8 Hz, H-12), 5.572 (1H, d, J = 14.8 Hz, H-12), 4.019 (3H, s, 6-OCH_3), 3.761 (3H, s, 7-OCH_3), 5.531 (1H, d, J = 3.6 Hz, H-1″), 4.516 (1H, d, J = 3.6 Hz, H-2″), 4.345 (1H, d, J = 9.7 Hz, H-4″), 3.932 (1H, d, J = 9.7 Hz, H-4″), 3.668 (1H, d, J = 11.4 Hz, H-5″), 3.710 (1H, d, J = 11.4 Hz, H-5″); $^{13}C\{^1H\}$ NMR (100 MHz, $CDCl_3$) δ 133.94 (s, C-1), 121.02 (s, C-2), 130.26 (s, C-3), 146.31 (s, C-4), 101.98 (d, C-5), 153.22 (s, C-6), 151.64 (s, C-7), 107.30 (d, C-8), 132.02 (s, C-9), 128.38 (s, C-10), 172.25 (s, C-11), 68.79 (t, C-12), 56.50 (q, OCH_3-6), 56.05 (q, OCH_3-7), 114.77 (s, C-1′), 98.94 (d, C-2′), 142.19 (s, C-3′), 149.80 (s, C-4′), 111.40 (d, C-5′), 150.79 (s, C-6′), 102.49 (t, C-7′), 112.82 (d, C-1″), 78.66 (d, C-2″), 80.31 (s, C-3″), 75.91 (t, C-4″), 64.23 (d, C-5″); CD (MeOH) λ ($\Delta\varepsilon$) 200 (−17.73), 212 (0.95), 217 (−0.34), 229 (9.36), 246 (−1.52), 262 (1.89), 276 (−2.36), 293 (−0.41), 315 (−2.03) nm.

*Justatropmer B (**2**) (Synthetic).* HRMS (ESI) m/z: $[M + H]^+$ calcd for $C_{26}H_{25}O_{12}$, 529.1346; found, 529.1331; ^1H NMR (CD_3OD, 400 MHz) δ_H 7.698 (1H, s, H-5), 7.076 (1H, s, H-8), 6.561 (1H, s, H-2′), 6.545 (1H, s, H-5′), 5.947 (1H, d, J = 1.0 Hz, H-7′), 5.969 (1H, d, J = 1.0 Hz, H-7′), 5.495 (1H, d, J = 14.8 Hz, H-12), 5.569 (1H, d, J = 14.8 Hz, H-12), 4.021 (3H, s, 6-OCH_3), 3.762 (3H, s, 7-OCH_3), 5.538 (1H, d, J = 3.6 Hz, H-1″), 4.518 (1H, d, J = 3.6 Hz, H-2″), 4.350 (1H, d, J = 9.7 Hz, H-4″), 3.934 (1H, d, J = 9.7 Hz, H-4″), 3.672 (1H, d, J = 11.4 Hz, H-5″), 3.713 (1H, d, J = 11.4 Hz, H-5″); $^{13}C\{^1H\}$ NMR (100 MHz, $CDCl_3$) δ 133.94 (s, C-1), 121.07 (s, C-2), 130.26 (s, C-3), 146.34 (s, C-4), 102.02 (d, C-5), 153.28 (s, C-6), 151.69 (s, C-7), 107.33 (d, C-8), 132.06 (s, C-9), 128.44 (s, C-10), 172.27 (s, C-11), 68.79 (t, C-12), 56.50 (q, OCH_3-6), 56.06 (q, OCH_3-7), 114.81 (s, C-1′), 98.98 (d, C-2′), 142.22 (s, C-3′), 149.83 (s, C-4′), 111.38 (d, C-5′), 150.88 (s, C-6′), 102.51 (t, C-7′), 112.84 (d, C-1″), 78.70 (d, C-2″), 80.31 (s, C-3″), 75.93 (t, C-4″), 64.28 (d, C-5″); CD (MeOH) λ ($\Delta\varepsilon$) 200 (23.17), 211 (−6.35), 218 (−3.32), 229 (−16.06), 246 (2.85), 260 (−4.02), 274 (4.66), 297 (−0.19), 313 (0.76) nm.

To a solution of **22b** (25.20 mg, 0.04 mmol) in THF/MeOH (1:3, 4 mL) was added $Pd(OH)_2$ on carbon (4 mg, 20%). The reaction was degassed 3 times with H_2 and stirred for 6 h under H_2 balloon. TLC showed the **22b** disappeared, and two new spots with higher polarity were formed. The mixture was purified by a silica gel column (PE/EtOAc 1:1) to afford compounds **23** (white powder, 8.23 mg, 43.3%) and **24** (white powder, 8.27 mg, 43.5%).

*Compound **23**.* HRMS (ESI) m/z: $[M + H]^+$ calcd for $C_{26}H_{25}O_{12}$, 529.1346; found, 529.1327; ^1H NMR (CD_3OD, 400 MHz) δ_H 8.001 (1H, s, H-5), 7.074 (1H, s, H-8), 6.560 (1H, s, H-2′), 6.552 (1H, s, H-5′), 5.938 (1H, d, J = 1.0 Hz, H-7′), 5.970 (1H, d, J = 1.0 Hz, H-7′), 5.585 (1H, d, J = 14.8 Hz, H-12), 5.506 (1H, d, J = 14.8 Hz, H-12), 4.037 (3H, s, 6-OCH_3), 3.791 (3H, s, 7-OCH_3), 5.482 (1H, d, J = 4.7 Hz, H-1″), 4.235 (1H, d, J = 4.7 Hz, H-2″), 4.203 (1H, d, J = 9.9 Hz, H-4″), 4.232 (1H, d, J = 9.9 Hz, H-4″), 3.645 (1H, d, J = 11.4 Hz, H-5″), 3.613 (1H, d, J = 11.4 Hz, H-5″); $^{13}C\{^1H\}$ NMR (100 MHz, $CDCl_3$) δ 133.88 (s, C-1), 121.02 (s, C-2), 130.56 (s, C-3), 146.70 (s, C-4), 102.48 (d, C-5), 153.20 (s, C-6), 151.68 (s, C-7), 107.08 (d, C-8), 132.04 (s, C-9), 129.12 (s, C-10), 172.33 (s, C-11), 68.82 (t, C-12), 56.64 (q, OCH_3-6), 56.03 (q, OCH_3-7), 114.83 (s, C-1′), 98.93 (d, C-2′), 142.18 (s, C-3′), 149.77 (s, C-4′), 111.35 (d, C-5′), 150.86 (s, C-6′), 102.90 (t, C-7′), 106.80 (d, C-1″), 76.68 (d, C-2″), 77.73 (s, C-3″), 73.80 (t, C-4″), 65.15 (d, C-5″); CD (MeOH) λ ($\Delta\varepsilon$): 200 (−29.98), 212 (11.95), 219 (6.87), 229 (24.50), 247 (−4.84), 263 (4.99), 275 (−6.53), 293 (−0.34), 313 (−1.44) nm.

*Compound **24**.* HRMS (ESI) m/z: $[M + H]^+$ calcd for $C_{26}H_{25}O_{12}$, 529.1346; found, 529.1331; ^1H NMR (CD_3OD, 400 MHz), δ_H 7.965 (1H, s, H-5), 7.073 (1H, s, H-8), 6.554 (1H, s, H-2′), 6.548 (1H, s, H-5′), 5.929 (1H, d, J = 1.0 Hz, H-7′), 5.965 (1H, d, J = 1.0 Hz, H-7′), 5.488 (1H, d, J = 14.8 Hz, H-12), 5.577 (1H, d, J = 14.8 Hz, H-12), 4.028 (3H, s, 6-OCH_3), 3.793 (3H, s, 7-OCH_3), 5.451 (1H, d, J = 4.6 Hz, H-1″), 4.218 (1H, d, J = 4.6 Hz, H-2″), 4.221 (1H, d, J = 9.9 Hz, H-4″), 4.195 (1H, d, J = 9.9 Hz, H-4″), 3.610(1H, d, J = 11.2 Hz, H-5″), 3.642 (1H, d, J = 11.2 Hz, H-5″); $^{13}C\{^1H\}$ NMR (100 MHz, $CDCl_3$) δ 133.83 (s, C-1), 121.00 (s, C-2), 130.52 (s, C-3), 146.62 (s, C-4), 102.47 (d, C-5), 153.14 (s, C-6), 151.62 (s, C-7), 107.08 (d, C-8), 131.98 (s, C-9), 129.03 (s, C-10), 172.31 (s, C-11), 68.81 (t, C-12), 56.63 (q, OCH_3-6), 56.02 (q, OCH_3-7), 114.80 (s, C-1′), 98.92 (d, C-2′), 142.15 (s, C-3′), 149.75 (s, C-4′), 111.41 (d, C-5′), 150.80 (s, C-6′), 102.84 (t, C-7′), 106.26 (d, C-1″), 76.68 (d, C-2″), 77.72 (s, C-3″), 73.80 (t, C-4″), 65.20 (d, C-5″); CD (MeOH) λ ($\Delta\varepsilon$): 200 (24.69), 212 (−0.50), 218 (0.808), 229 (−11.93), 246 (1.61), 262 (−3.42), 275 (4.40), 291 (1.36), 314 (2.82) nm.

Cells and Plasmids. The HIV vector pNL4-3.Luc.R-.E- was obtained from the AIDS Research and Reference Program, Division of AIDS, NIAID, NIH (Rockville, MD). The plasmid pHEF-VSV-G was kindly provided by Dr Lijun Rong (University of Illinois at Chicago, Chicago, IL).

Human lung epithelial cell line A549 and human embryonic kidney cell line 239T were cultured in DMEM supplemented with 10% (v/v) fetal bovine serum, 100 μg/mL of streptomycin and 100 units/mL of penicillin (all Gibco, Carlsbad, CA) at 37 °C and 5% CO_2.

Anti-HIV Activity Assay. HIV/VSV pseudovirions were prepared by using the same protocol described previously.[6] The antiviral evaluation assay was adopting the same protocol described in our previous study.[6] Briefly, target A549 cells were seeded in 96-well plates at a density of 4000 cells/well 24 h before infection. The tested compounds were added in the 96-well plates together with the viruses at various concentrations in 0.5% DMSO (v/v). The wells treated with viruses alone with 0.5% DMSO were used as negative controls, and the wells treated azidothymidine (AZT) were used as positive controls. Each compound was tested in triplicate in three independent experiments. Inhibitory concentrations 50% (IC_{50}) and cytotoxic concentrations 50% (CC_{50}) were calculated using GraphPad Prism Software (version 6, La Jolla, CA).

Scan the Rotation Barrier of the 6′-Hydroxy-Substituted in 6′-Hydroxyusticidin B and the Aglycone of Justatropmers. Molecular Merck force field (MMFF) and DFT/TDDFT calculations were performed with the Spartan 14 software package (Wavefunction Inc., Irvine, CA) and Gaussian16 program package,[36] respectively, using default grids and convergence criteria. MMFF conformational search generated low-energy conformers within a 10 kcal/mol energy window were subjected to geometry optimization using the B3LYP/6-31G(d) method. Based on the input structures of 6′-hydroxyjusticidin B, the aglycones of justatropmer rotational energy barriers were

https://doi.org/10.1021/acs.joc.1c00068
J. Org. Chem. 2021, 86, 5568−5583

determined from relaxed dihedral angle scans that were performed with the program Gaussian16 employing the B3LYP/6-31G(d) method with a torsion angle increment of 5°. The structures were optimized prior to the torsion scan using the same level of theory.

The axial rotation barrier energy of 6′-hydroxyjusticidin B was estimated as 34.8 kcal/mol (Figure S1B), and the axial rotation barrier energy of the aglycone of justatropmers was also estimated as 34.8 kcal/mol (Figure S1C). Further optimization of the rotational transition state structures were carried out at the B3LYP-D3(BJ)/6-311+G(d,p)-SMD (MeOH)/B3LYP/6-31G(d) level, which yielded 26.3 and 26.5 kcal/mol for 6′-hydroxyjusticidin B and aglycone, respectively (Figure S1D,E).

Computational Section. The rotation barriers of dihedral angle (C2−C1−C1′−C2′) in 6′-hydroxyjusticidin B and the aglycone of justatropmers were calculated based on the simplified model of the crystallographic structure of **5**, in which the sugar residue at C-4 was removed. The relaxed dihedral angle scans were performed by the program Gaussian16[36] employing the B3LYP/6-31G(d) method with a torsion angle increment of 5°. The same axial rotation barrier energies, which was estimated as 34.8 kcal/mol, were found for both 6′-hydroxyjusticidin B (Figure S1B) and aglycone of justatropmers (Figure S1C), suggesting that the hydroxyl group at C-4 has a negative effect for the rotation barrier.

For aglycone of **1**, the initial structure was the conformer of the lowest energy during the rotation barrier scan. A geometry optimization and frequency calculation were recalculated at B3LYP/6-31G(d). Then 32 excited states were taken into consideration for TDDFT calculations at M06-2X/def2TZVP.

The ECD calculation of (1′***P***)-**9** was processed as follows: Molecular Merck force field (MMFF) was performed with Spartan 14 software package (Wavefunction, Inc., Irvine, CA) using default grids and convergence criteria. In detail, MMFF conformational search generated low-energy conformers within a 10 kcal/mol energy window were subjected for further geometry optimization by the B3LYP/6-31G(d) method. Frequency calculations were then carried out using the same method to verify that each optimized conformer was a true minimum. The single-point energies of the optimized conformers were recalculated at the M06-2X/def2TZVP level. Thus, the Gibbs free energy, obtained by the sum of single-point energy at M06-2X/def2TZVP and the thermal correction at B3LYP/6-31G(d), was used for the relative thermal free energy (DG) calculation and following Boltzmann population analysis at 298.15 K. All the conformers of (1′***P***)-**9** were taken into account for the following TDDFT calculations.

The TDDFT calculations for (1′***P***)-**9** conformers were performed using the M06-2X, ωB97X-D, and CAM-B3LYP functionals with basis set def2TZVP. The number of excited states per each molecule was set to 32. The ECD spectra were generated by the program SpecDis[37] using a Gaussian band shape from dipole-length dipolar and rotational strengths. The calculated spectra were finally generated from the Boltzmann weighting of each conformer.

It should be noted that the Grimme's dispersion (D3 version) was used for empirical dispersion correction (except for the ωB97X-D method). Solvent effects (in MeOH) were taken into account by using the default SCRF method integral equation formalism variant (IEFPCM) for the whole calculation.

■ ASSOCIATED CONTENT

Supporting Information

The Supporting Information is available free of charge at https://pubs.acs.org/doi/10.1021/acs.joc.1c00068.

For details regarding axial rotation barrier energy and UV, IR, HRESMS, NMR, and CD spectra for the compounds **1**−**12**; HRESMS, MS, and NMR spectra were obtained for the synthetic compounds (**14**, **15**, **18**−**24**, **1**, and **2**) (PDF)

Accession Codes

CCDC 1974784 contains the supplementary crystallographic data for this paper. These data can be obtained free of charge via www.ccdc.cam.ac.uk/data_request/cif, or by emailing data_request@ccdc.cam.ac.uk, or by contacting The Cambridge Crystallographic Data Centre, 12 Union Road, Cambridge CB2 1EZ, UK; fax: +44 1223 336033.

■ AUTHOR INFORMATION

Corresponding Author

Hong-Jie Zhang − *School of Chinese Medicine, Hong Kong Baptist University, Kowloon Tong, Hong Kong SAR, People's Republic of China*; orcid.org/0000-0002-7175-5166; Email: zhanghj@hkbu.edu.hk

Authors

Yang Zhao − *School of Chinese Medicine, Hong Kong Baptist University, Kowloon Tong, Hong Kong SAR, People's Republic of China*

Chuen-Fai Ku − *School of Chinese Medicine, Hong Kong Baptist University, Kowloon Tong, Hong Kong SAR, People's Republic of China*

Xin-Ya Xu − *School of Chinese Medicine, Hong Kong Baptist University, Kowloon Tong, Hong Kong SAR, People's Republic of China*

Nga-Yi Tsang − *School of Chinese Medicine, Hong Kong Baptist University, Kowloon Tong, Hong Kong SAR, People's Republic of China*

Yu Zhu − *School of Chinese Medicine, Hong Kong Baptist University, Kowloon Tong, Hong Kong SAR, People's Republic of China*

Chen-Liang Zhao − *School of Chinese Medicine, Hong Kong Baptist University, Kowloon Tong, Hong Kong SAR, People's Republic of China*

Kang-Lun Liu − *School of Chinese Medicine, Hong Kong Baptist University, Kowloon Tong, Hong Kong SAR, People's Republic of China*

Chuang-Chuang Li − *Shenzhen Grubbs Institute and Department of Chemistry, Southern University of Science and Technology, Shenzhen 518055, People's Republic of China*; orcid.org/0000-0003-4344-0498

Lijun Rong − *Department of Microbiology and Immunology, College of Medicine, University of Illinois at Chicago, Chicago, Illinois 60612, United States*

Complete contact information is available at: https://pubs.acs.org/10.1021/acs.joc.1c00068

Notes

The authors declare no competing financial interest.

■ ACKNOWLEDGMENTS

The work described in this paper was supported by the Research Grant Council of the Hong Kong Special Administrative Region, China (Projects No. HKBU 12103618 and 12103917), the Innovation and Technology Commission of Hong Kong Special Administrative Region, China (MHP/105/19), and the Hong Kong Scholars Program Foundation (NO. XJ2017058). We are grateful to Dr. Liu Kai from Institute of Marine Drugs, Guangxi University of Chinese Medicine, for assistance with the ECD calculations and Professor Pei-Yuan Yu, Department of Chemistry, Southern University of Science and Technology, for assistance with the calculation of the barriers between the two atropisomers.

REFERENCES

(1) Teponno, R. B.; Kusari, S.; Spiteller, M. Recent advances in research on lignans and neolignans. *Nat. Prod. Rep.* **2016**, *33*, 1044−1092.

(2) Day, S. H.; Lin, Y. C.; Tsai, M. L.; Tsao, L. T.; Ko, H. H.; Chung, M. C.; Lee, J. C.; Wang, J. P.; Won, S. J.; Lin, C. N. Potent cytotoxic lignans from *Justicia procumbens* and their effects on nitricoxide and tumor necrosis factor-α production in mouse macrophages. *J. Nat. Prod.* **2002**, *65*, 379−381.

(3) Day, S. H.; Chiu, N. Y.; Tsao, L. T.; Wang, J. P.; Lin, C. N. New lignan glycosides with potent antiinflammatory effect, isolated from *Justicia ciliata*. *J. Nat. Prod.* **2000**, *63*, 1560−1562.

(4) Weng, J. R.; Ko, H. H.; Yeh, T. L.; Lin, H. C.; Lin, C. N. Two new arylnaphthalide lignans and anti-platelet constituents from *Justicia procumbens*. *Arch. Pharm.* **2004**, *337*, 207−212.

(5) Asano, J.; Chiba, K.; Tada, M.; Yoshii, T. Antiviral activity of lignans and their glycosides from *Justicia Procumbens*. *Phytochemistry* **1996**, *42*, 713−717.

(6) Zhang, H. J.; Rumschlag-Booms, E.; Guan, Y. F.; Wang, D. Y.; Liu, K. L.; Li, W. F.; Nguyen, V. H.; Cuong, N. M.; Soejarto, D. D.; Fong, H. S.; Rong, L. J. Potent inhibitor to drug-resistant HIV-1 strains identified from the medicinal plant *Justicia gendarussa*. *J. Nat. Prod.* **2017**, *80*, 1798−1807.

(7) Zhang, H. J.; Rumschlag-Booms, E.; Guan, Y. F.; Liu, K. L.; Wang, D. Y.; Li, W. F.; Nguyen, V. H.; Cuong, N. M.; Soejarto, D. D.; Fong, H. S.; Rong, L. J. Anti-HIV diphyllin glycosides from *Justicia gendarussa*. *Phytochemistry* **2017**, *136*, 94−100.

(8) Martinez-Lopez, A.; Persaud, M.; Chavez, M. P.; Zhang, H. J.; Rong, L. J.; Liu, S. F.; Wang, T. T.; Sarafianos, S. G.; Diaz-Grifferoa F, F. Glycosylated diphyllin as a broad-spectrum antiviral agent against Zika virus. *EBioMed.* **2019**, *47*, 269−283.

(9) Mancinelli, M.; Bencivenni, G.; Pecorari, D.; Mazzanti, A. Stereochemistry and recent applications of axially chiral organic molecules. *Eur. J. Org. Chem.* **2020**, 4070−4086.

(10) Charlton, J. L.; Oleschuk, C. J.; Chee, G. L. Hindered rotation in arylnaphthalene lignans. *J. Org. Chem.* **1996**, *61*, 3452−3457.

(11) Wolf, C.; Pirkle, W. H.; Welch, C. J.; Hochmuth, D. H.; Konig, W. A.; Chee, G. L.; Charlton, J. L. Determination of the enantiomerization barrier of arylnaphthalene lignans by cryogenic subcritical fluid chromatography and computer simulation. *J. Org. Chem.* **1997**, *62*, 5208−5210.

(12) Oki, M. *Recent advances in atropisomerism in topics in stereochemistry*; John Wiley & Sons, Inc., 1983; pp 1−81.

(13) Smyth, J. E.; Butler, N. M.; Keller, P. A. A twist of nature−the significance of atropisomers in biological systems. *Nat. Prod. Rep.* **2015**, *32*, 1562−1583.

(14) Leroux, F. Atropisomerism, biphenyls, and fluorine: a comparison of rotational barriers and twist angles. *ChemBioChem* **2004**, *5*, 644−649.

(15) Wang, S. P.; Tong, Y. F.; Li, L.; Wu, S.; Qi, Y. The synthesis of justicidinoside B and its atropisomer. *J. Asian Nat. Prod. Res.* **2013**, *15*, 644−649.

(16) Rezanka, T.; Rezanka, P.; Sigler, K. Glycosides of arylnaphthalene lignans from *Acanthus mollis* having axial chirality. *Phytochemistry* **2009**, *70*, 1049−1054.

(17) Di Maso, M. J.; Grove, C. I.; Shaw, J. T. Studies in the synthesis of biaryl natural products: the 6, 6′-binaphthopyranones. *Strategies and Tactics in Organic Synthesis* **2014**, *10*, 225−248.

(18) Singh, J.; Hagen, T. J. Chirality and biological activity. *Drug Discovery* **2010**, *5*, 127−166.

(19) Laplante, S. R.; Edwards, P. J.; Fader, L. D.; Jakalian, A.; Hucke, O. Revealing atropisomer axial chirality in drug discovery. *ChemMedChem* **2011**, *6*, 505−513.

(20) Laplante, S. R.; Fader, L. D.; Fandrick, K. R.; Fandrick, D. R.; Hucke, O.; Kemper, R.; Miller, S. P. F.; Edwards, P. J. Assessing atropisomer axial chirality in drug discovery and development. *J. Med. Chem.* **2011**, *54*, 7005−7022.

(21) Castellanos, S.; López-Calahorra, F.; Brillas, E.; Julil, L.; Velasco, D. All-organic discotic radical with a spin-carrying rigid-core showing intracolumnar interactions and multifunctional properties. *Angew. Chem., Int. Ed.* **2009**, *48*, 6516−6519.

(22) Zhao, C.; Rakesh, K. P.; Mumta, z S.; Moku, B.; Asiri, A. M.; Manukumar, H. M.; Qin, H. L. Arylnaphthalene lactone analogues: synthesis and development as excellent biological candidates for future drug discovery. *RSC Adv.* **2018**, *8*, 9487−9502.

(23) Yang, M. H.; Wu, J.; Cheng, F.; Zhou, Y. Complete assignments of ^{1}H and ^{13}C NMR data for seven arylnaphthalide lignans from *Justicia procumbens*. *Magn. Reson. Chem.* **2006**, *44*, 727−730.

(24) Perdew, J. P.; Burke, K.; Ernzerhof, M. Generalized gradient approximation made simple. *Phys. Rev. Lett.* **1996**, *77*, 3865−3868.

(25) Adamo, C.; Barone, V. Toward reliable density functional methods without adjustable parameters: The PBE0 mode. *J. Chem. Phys.* **1999**, *110*, 6158−6169.

(26) Staroverov, V. N.; Scuseria, G. E.; Tao, J.; Perdew, J. P. Comparative assessment of a new nonempirical density functional: Molecules and hydrogen-bonded complexes. *J. Chem. Phys.* **2003**, *119*, 12129−12137.

(27) Rumschlag-Booms, E.; Zhang, H. J.; Soejarto, D. D.; Fong, H. H. S.; Rong, L. J. Development of an antiviral screening protocol: One-Stone-Two-Birds. *J. Antivirals Antiretrovirals* **2011**, *3*, 008−010.

(28) Gözler, B.; Gözler, T.; Sağlam, H.; Hesse, M. Minor lignans from *Haplophyllum cappadocicum*. *Phytochemistry* **1996**, *42*, 689−693.

(29) Sheriha, G. M.; Amer, K. A. Lignans of *Haplophyllum tuberculatum*. *Phytochemistry* **1984**, *23*, 151−153.

(30) Superchi, S.; Scafato, P.; Gorecki, M.; Pescitelli, G. Absolute configuration determination by quantum mechanical calculation of chiroptical spectra: basics and applications to fungal metabolites. *Curr. Med. Chem.* **2018**, *25*, 287−320.

(31) Srebro-Hooper, M.; Autschbach, J. Calculating natural optical activity of molecules from first principles. *Annu. Rev. Phys. Chem.* **2017**, *68*, 399−420.

(32) Pescitelli, G.; Bruhn, T. Good computational practice in the assignment of absolute configurations by TDDFT calculations of ECD spectra. *Chirality* **2016**, *28*, 466−474.

(33) Mancinelli, M.; Franzini, R.; Renzetti, A.; Marotta, E.; Villani, C.; Mazzanti, A. Determination of the absolute configuration of conformationally flexible molecules by simulation of chiro-optical spectra: a case study. *RSC Adv.* **2019**, *9*, 18165−18175.

(34) Patel, D. C.; Woods, R. M.; Breitbach, Z. S.; Berthod, A.; Armstrong, D. W. Thermal racemization of biaryl atropisomers. *Tetrahedron: Asymmetry* **2017**, *28*, 1557−1561.

(35) Xiong, L.; Bi, M. G.; Wu, S.; Tong, Y. F. Total synthesis of 6′-hydroxyjusticidin A. *J. Asian Nat. Prod. Res.* **2012**, *14*, 322−326.

(36) Frisch, M. J.; Trucks, G. W.; Schlegel, H. B.; Scuseria, G. E.; Robb, M. A.; Cheeseman, J. R.; Scalmani, G.; Barone, V.; Petersson, G. A.; Nakatsuji, H.; Li, X.; Caricato, M.; Marenich, A. V.; Bloino, J.; Janesko, B. G.; Gomperts, R.; Mennucci, B.; Hratchian, H. P.; Ortiz, J. V.; Izmaylov, A. F.; Sonnenberg, J. L.; Williams-Young, D.; Ding, F.; Lipparini, F.; Egidi, F.; Goings, J.; Peng, B.; Petrone, A.; Henderson, T.; Ranasinghe, D.; Zakrzewski, V. G.; Gao, J.; Rega, N.; Zheng, G.; Liang, W.; Hada, M.; Ehara, M.; Toyota, K.; Fukuda, R.; Hasegawa, J.; Ishida, M.; Nakajima, T.; Honda, Y.; Kitao, O.; Nakai, H.; Vreven, T.; Throssell, K.; Montgomery, J. A., Jr.; Peralta, J. E.; Ogliaro, F.; Bearpark, M. J.; Heyd, J. J.; Brothers, E. N.; Kudin, K. N.; Staroverov, V. N.; Keith, T. A.; Kobayashi, R.; Normand, J.; Raghavachari, K.; Rendell, A. P.; Burant, J. C.; Iyengar, S. S.; Tomasi, J.; Cossi, M.; Millam, J. M.; Klene, M.; Adamo, C.; Cammi, R.; Ochterski, J. W.; Martin, R. L.; Morokuma, K.; Farkas, O.; Foresman, J. B.; Fox, D. J. *Gaussian 16*, revision C.01; Gaussian, Inc.: Wallingford, CT, 2016.

(37) Bruhn, T.; Schaumlöffel, A.; Hemberger, Y.; Bringmann, G. SpecDis: quantifying the comparison of calculated and experimental electronic circular dichroism spectra. *Chirality* **2013**, *25*, 243−249.

NOTE ADDED AFTER ASAP PUBLICATION

Figure S6 in the Supporting Information was corrected on April 6, 2021.

https://doi.org/10.1021/acs.joc.1c00068
J. Org. Chem. 2021, 86, 5568−5583